# **Microgrid-Shaped Diamond Crystals From Alternating Current 50 Hz Sputtering-Assisted**Chemical Vapour Deposition

Vittaya Amornkitbamrung

Department of Physics, Faculty of Science, Khon Kaen University, Friendship Highway, Khon Kaen 40002, Thailand.

Alternating current (a.c.) 50 Hz sputtering-assisted chemical vapour deposition method from methane gas was used to deposit diamond thin films on (100) diamond substrates. It is the first time "microgrid-shaped" diamond crystals similar to a beehive were observed. Field emission scanning electron microscopy (FE-SEM) at 5 kV accelerating incident electron beam was used to observe surface morphology of thin films and crystallites. Laser Raman microprobe spectroscopy was used to confirm the chemical structure of thin films and crystallites. The Raman peak of a microgrid-shaped diamond crystal was at 1332.35 cm<sup>-1</sup>; 0.50 cm<sup>-1</sup> higher than the diamond substrate Raman peak which is at 1331.85 cm<sup>-1</sup>. This may be caused by strain in microgrid-shaped diamond. Using laser beam scanning over all of the sample surface showed diamond Raman peak only; no graphite Raman peak was detected.

The surface energy of diamond is higher than other semiconducting materials i.e. Si, Ge because diamond has the shortest nearest neighbor interatomic distance. Diamond has a surface energy (3.7 joule/m²) higher than graphite (3.1 joule/m²) for equilibrium with carbon vapour. It is necessary to heat the diamond surface during homoepitaxial diamond deposition by some methods such as hot wire filament in front of the diamond surface or by a heated plate underneath the diamond substrate. These heating methods may lead to contamination of the diamond substrate from heating components. A heating method which does not contaminate the surface is using infrared radiation from CO<sub>2</sub> laser, but it is not easy to approach high temperatures around 1000 ° C on the diamond surface because of high thermal conductivity of diamond. It transfers heat from front surface to back rapidly.

This report presents about the deposition of diamond thin films achieved by using a simple a.c. sputtering assisted chemical vapour deposition (CVD) system which was developed at my laboratory. There are two graphite electrodes which are in horizontal orientation. The substrate face is inclined at about 45° to the gas flowed direction and off-axis of the graphite electrodes. The argon and methane gases were flowed from the opposite side of the substrate. This configuration set-up has important phenomena i.e. it is etching all the time with C+ and H+ during the CVD process and the mixed gases which are not discharged by a.c. high voltage will be reflected from the diamond surface and pumped out through the vacuum pump line. The graphite electrodes have two actions i.e. cleaning electrodes for argon ion etching and supplying a carbon source for saturated conditions for diamond deposition. This is a flexible system for surface treatment and thin film deposition. A more detailed set-up will be published in the near future. Briefly this set-up has essential monitors for deposition experiments such as mass flow meters, "in situ" thickness measurement, optical pyrometer and residual gas analyzer, etc.

Diamond (100) face of 1.5 mm x 1.5 mm x 0.3 mm size was used as the substrate for the diamond thin film deposition. Before a substrate was loaded into the load-lock system, it was etched by boiling in mixed acid, i.e.,  $H_2SO_4$ :  $HNO_3 = 9:1$  by volume for 1 h (the same method as that used by Ando *et al.*<sup>(2)</sup>), washed with 18 mega-ohm-cm ultrapure water, and blown dry by pure nitrogen gas.

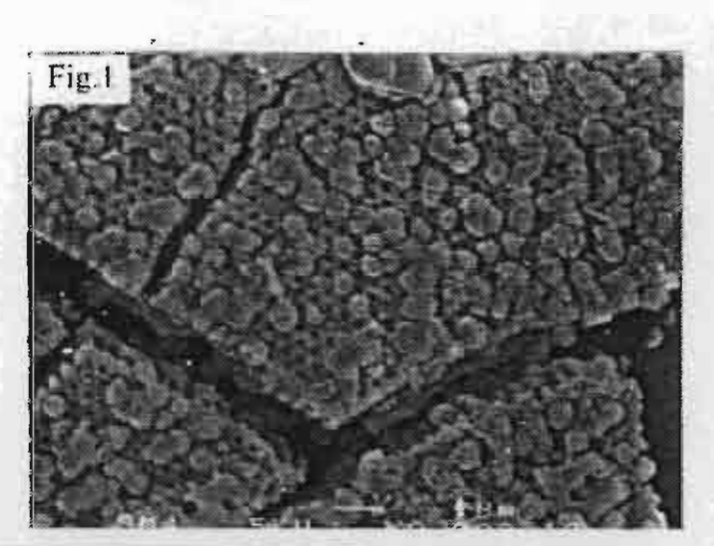
The diamond substrate was loaded into the load-lock chamber which was evacuated by turbomolecular pump under pressure from the growth chamber of  $2.7 \times 10^8$  millibar. The diamond substrate was transferred into the center of the growth chamber through the gate valve. Before the CVD process started, the diamond surface was etched with argon ions for 15 minutes. The growth

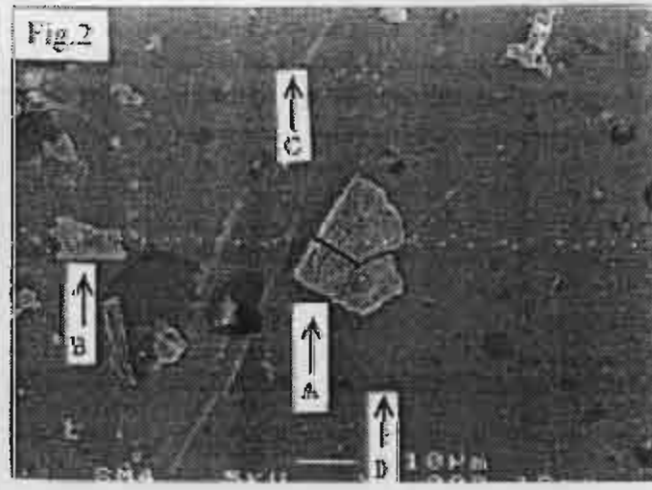
condition parameters were 2x10<sup>-1</sup> millibar, 10 hours deposition time with a.c. 50 Hz sputtering assisted chemical vapour depisition from methane gas during glow discharge by a.c. power, 3.2 kV, 38 mA.

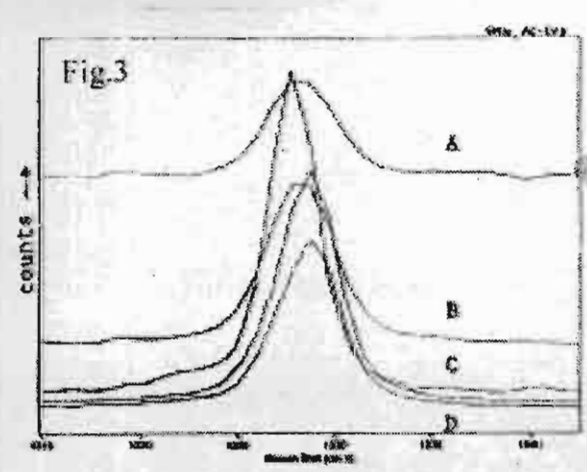
Laser Raman microprobe spectrometer with reflected optical microscope was used to detect the Raman spectrograph in the same area as the "microgrid-shaped" diamond crystals similar to a "beehive", as shown in FE-SEM image in Fig. 1. The Raman spectrographs from 4 different points (A,B,C, and D) from FE-SEM image are shown in Fig. 2, and overlayed with standard(std) diamond Raman spectrograph showing small shifts as shown in Fig. 3. The peak position has been measured at the position of the centre at the full width at half maximum intensity (FWHM). The 4 different points give Raman peaks of points A,B,C, and D at 1332.35, 1332.10, 1332.72, and 1332.72 cm<sup>-1</sup> respectively. The FWHM of Raman peaks of points A,B,C, and D are 4.25, 4.25, 3.62, and 3.62 cm<sup>-1</sup> respectively. The standard diamond gives a Raman peak at 1331.85 cm<sup>-1</sup>, and FWHM is 3.0 cm<sup>-1</sup>. Small shifts in the band wavenumber have been related to the stress state of crystallites and deposited films.

### REFERENCES

- 1. V. Amornkitbamrung: New Diamond and Frontier Carbon Technology Vol.9, No.4 (1999) xxx. (in press).
- 2. T. Ando, H. Haneda, M. Akaishi, Y. Sato and M. Kamo: Diamond Relat. Mater. Vol.5 (1996) 34.







# Th International Contact Harman May District

23-28 July 2000

City University of Hong Kong,

Hong Kong

# PROGRAM & ABSTRACTS

Japan New Diamond



開金川市製 海道(Mitthub contex Of SuparaDlamone



香港城市大學 etty University of Honor Konor

### Session 15: Posters & Mini-trade Exhibition

### Chairmen:

C.S. Lee (City University of Hong Kong, Hong Kong), L.K.Y. Li (City University of Hong Kong, Hong Kong)

### Session 15A: Growth and Processing

15a.1	111-Oriented Growth of Diamond on Ir/CaF <sub>2</sub> /Si(111) Substrates by Electron Cyclotron Resonance Nucleation and ,Microwave Plasma Assisted Chemical Vapor Deposition. <u>C. H. Lee, L. S. Hung, I. Bello and S. T. Lee</u> (COSDAF, University of Hong Kong, Hong Kong)
15a.2	Analysis of Carbon Conversion Efficiency and Heat Transfer Characteristics in Microwave-Assisted Diamond Chemical Vapor Deposition  D. S. Dandy <sup>1</sup> , R. Campbell, <sup>2</sup> J. E. Butler <sup>3</sup> and A. Srinivasan <sup>2</sup> ( <sup>1</sup> Colorado State University, USA), ( <sup>2</sup> Geo-Centers, Inc., USA),  ( <sup>3</sup> Naval Research Laboratory, USA)
15a.3	Charged Cluster Model as a Growth Mechanism of CVD Diamond N.M. Hwang <sup>1,2</sup> , I.D. Jeon <sup>1</sup> , H.S. Ahni <sup>1</sup> and D.Y. Kim <sup>1</sup> ( <sup>1</sup> Seoul National University, South Korea), ( <sup>2</sup> Korea Research Institute of Standards and Science, South Korea)
15a.4	Diamond Films Grown by a 60 kW Microwave Plasma CVD System  T. Tachibana <sup>1</sup> , Y. Ando <sup>1</sup> , A. Watanabe <sup>1</sup> , Y. Nishibayashi <sup>1</sup> , K. Kobashi <sup>1</sup> , T. Hirao <sup>2</sup> and K. Oura <sup>2</sup> ( <sup>1</sup> FCT Project/JFCC, Japan)  ( <sup>2</sup> Osaka University, Japan)
15a.5	Diamond Single Crystals Kinetic Growth with Using of a Set Seeds S. A. Ivakhnenko, O. A. Zanevsky, I. S. Belousov (Institute for Superhard Materials Ukrainian Academy of Sciences, Ukraine)
15a.6	Diamond Synthesis on Large Area of Silicon Substrate by a Combination Method B. Y. Miao, Q. Huang, B. Zhang, L. J. Fan, Q. J. Zheng (Southeast University, Nanjing)
15a.7	Early Stages of Diamond Growth on an Epitaxied Ir Layer Studied by Electron Spectroscopies (AES, XPS).  J. C. Arnault, S. Pecoraro and F. L. Normand (Institute de Physique et Chimie de Strasbourg, France)
15a.8	Effect of Substrate Holder Boundaries on Diamond Nucleation by Biasing in Microwave Plasma Chemical Vapor Deposition T. Sharda, T. Soga, T. Jimbo and M. Umeno (Nagoya Institute of Technology, Japan)
15a.9	First Stages of Diamond Nucleation on Iridium F. Hörmann, H. Roll, M. Schreck and B. Stritzker (Universität Augsburg, Institut Für Physik, Germany)
15a.10	Hot Filament Chemical Vapor Deposition of Diamond Films on Ion-beam nitrided Steel N. G. Shang, Z. F. Zhou, C. S. Lee, I. Bello, S. T. Lee (COSDAF, City University of Hong Kong, Hong Kong)
<u>15a.11</u>	Hot Filament Chemical Vapor Deposition and Alternating Current Assisted Chemical Vapor  Deposition for Diamond Thin Film Production  V. Amornkitbamrung (Khon Kaen University, Kohon Kaen)

### Abstract 15a.11

# Hot filament chemical vapour deposition and alternating current assisted chemical vapour deposition for diamond thin film production

V. Amornkitbamrung

Department of Physics, Faculty of Science, Khon Kaen University, Thailand
40002, Thailand. email:vittaya@kkul.kku.ac.th

In this study, a system for the efficient production pf diamond thin films is developed. Films can be produced both by hot filament chemical vapour deposition (HF-CVD) and alternating current assisted chemical vapour deposition (AC-CVD), or by a hybrid of the two methods at the same time. It is a system that can measure the partial pressure of mixed gases, such as methane, hydrogen and oxygen. The sample can also be changed without disrupting vacuum because it corporates a load-lock system. The temperature of the hot filament and the substrate can be measured extenally using an optical pyrometer, thus enabling greater variatin of parameters such as temperature, pressure, ratio of gas flows and constitution of gas mixture. This will allow the reproducible production of diamond thin films in this future. Thirty-one diamond thin film samples were prepared in this project. It was found that the production of thin film on diamond substrate by vapour-phase epitaxy (VPE) depends on the thickness of oxide layer and the method of the oxide layer removal. However since the number of samples is small, the optimal parameters for complete epitaxy have not been found. More samples must be prepared in order to remove finely tune the parameters that are involved in find the optimum set of parameters.

Key words: hot filament, alternating current, chemical vapour deposition, thin film diamond, homoepitaxial, vapour-phase epitaxy, XPS, Raman, SEM

Hot Filament Chemical Vapour Deposition and Alternating Current Assisted Chemical Vapour Deposition for Diamond Thin Film Production

Vittaya Amornkitbamrung, Ong-On Topon and Wirat Jarernboon Department of Physics, Faculty of Science, Khon Kaen University, Khon Kaen 40002, Thailand

email:vittaya@kku1.kku.ac.th, Phone: (66)(43)246534-39ext.2248, Fax: (66)(43)244416

Keywords: hot filament, alternating current, chemical vapour deposition, thin film, diamond, DLC, homoepitaxial, vapour-phase epitaxy, XPS, Raman, SEM Abstract

In this study a system for the efficient production of diamond and diamond-like carbon (DLC) thin film is produced. Films can be produced both by hot filament chemical vapour deposition (HF-CVD) and alternating current assisted chemical vapour deposition (AC-CVD), or by a hybrid of the two methods at the same time. It is a system that can measure the partial pressure of mixed gases, such as methane, hydrogen and oxygen. The sample can also be changed without disrupting vacuum because it incorporates a loadlock system. The temperature of the hot filament and the substrate can be measured externally using an optical pyrometer, thus enabling greater variation of parameters such as temperature, pressure, ratio of gas flows and constitution of gas mixture. This will allow the reproducible production of diamond and DLC thin films in the future. Thirtyone diamond thin film and twenty DLC thin film samples were prepared in this project. It was found that the production of diamond thin film on diamond substrate by vapour phase epitaxy (VPE) depends on the amount of oxide layer and the method of removing the oxide layer. The quality of DLC thin film depends on the chemical etching time. However since the number of samples is small, the optimal parameters for complete epitaxy and high quality DLC thin film have not yet been found. More samples must be prepared in order to more finely tune the parameters that are involved to find the optimum set of parameters.

### 1. Introduction

There are many techniques[1] which have succeeded in diamond and DLC thin film preparation such as chemical vapour deposition(CVD) from hydrocarbon gas cracking by using microwave, r.f., hot filament energy sources; or a.c., d.c. sputtering from graphite target and carbon ion beam deposition. The r.f. hydrocarbon gas discharge technique[2] gives DLC films which have some impurity contamination from electrode material. Ion beam techniques[3] can eliminate impurities by using sophisticated technology. The present authors introduced a simple hybrid alternative method composed of a.c. 50 Hz sputtering from dual graphite targets and chemical vapour deposition from CH<sub>4</sub>: H<sub>2</sub> mixed gas, is called AC-CVD; and hot filament chemical vapour deposition, is called HF-CVD. The a.c. 50 Hz sputtering is similar to the method of Koinuma et al.[4] using for

deposition of high T<sub>C</sub> superconducting thin films. The a.c. 50 Hz sputtering technique was used successfully in deposition of DLC on various substrates[5] and the a.c. 50 Hz sputtering-MPCVD hybrid technique has succeeded in deposition of DLC on ZnSe infrared windows[6]. In this paper we discuss the sputtering-CVD hybrid system growth procedures; the compositional characterization of films on Si and diamond substrates; surface morphology by scanning electron microscope. The influence of the argon ions etching the diamond surface and chemical etching Si surface on the growth process is also discussed.

### 2. Experimental details

Plan view diagram of the a.c. 50 Hz sputtering-CVD hybrid system is shown in Fig.1. The 12 inch diameter cylindrical growth chamber was made of stainless steel type no. 316. In this system we flow all processing gases in the horizontal manner. In this experiment we introduced a substrate holder guide rod also made of stainless steel horizontally too. The substrate holder plate was made of high purity gold to reduce impurity contamination, especially oxide species. We monitored the substrate temperature by the chromel-alumel thermocouples. The thickness monitor was close to the substrate position to measure the suitable growth condition for diamond deposition. We detected the relative partial pressures of gases such as H<sub>2</sub>, CH<sub>4</sub>, and O<sub>2</sub> during processing by sampling gas from the growth chamber through a bypass fine metering control valve.

The diamond substrates, (100) orientation face with size 2.5 mm x 2.5 mm x 0.3 mm in size, type Ib (Sumitomo Electric Co., Japan) were first solvent-cleaned using acetone and methanol in an ultrasonic water bath, and rinsed with deionized (18 Megaohm-cm) water. The substrates were dried in a stream of nitrogen gas. After solvent-cleaning treatment, the substrates were treated in boiling mixtures of H<sub>2</sub>SO<sub>4</sub> and HNO<sub>3</sub>, 9:1 by volume, for 1 hour the same as a work of Ando et al. [7] to remove metallic and graphite impurities, then washed thoroughly in deionized (18 Megaohm-cm) water.

The Si (100) wafer, 25.4 mm in diameter and 0.45 mm in thickness, was sectioned into specimens 10 mmx 10 mm and cleaned with acetone and methanol in an ultrasonic cleaner for 1 h in each solvent, rinsed with deionized water and dried with dry nitrogen. The clean Si substrate was etched with lactic acid: HNO<sub>3</sub>: HF by volume for 10 minutes and rinsed with deionized water until neatralized, then dried with dry nitrogen.

The growth chamber was evacuated by combined turbomolecular and titanium pump until the ultimate pressure of about 10<sup>-8</sup> torr. The substrate was loaded into the load-lock chamber which was evacuated by turbomolecular pump. The substrate was

transferred into the center of the growth chamber through the gate valve. The growth condition parameters of some samples are summarized in Table 1.

### 3. Results and Discussion

Fig.2 (a), (b) show the surface morphology from SEM images. For AC-CVD process, Fig.2(a) shows the facet edges which are registered along the same directions for different flat crystals. Hence, the growth is epitaxial, not ramdomly seeded. For HF-CVD process, Fig.2 (b) shows a diamond crystal which has a facet edge parallel to the substrate.

X-Ray Photoelectron Spectroscopy (XPS) was used to study the diamond surface before and after diamond deposition by AC-CVD and HF-CVD methods. The XPS results were comparative analyzed with other works [8-13] are summarized in Table 2. The important peaks are at 284-285 eV, 286.8 eV and and 288 eV for C-C, C-OH, and C-O bonding, respectively. XPS results are shown in Fig. 3. HF-CVD shows C1s peak at about 285 eV. There is no significant difference between 30 and 60 minutes heat treatment of substrate surface at 4x10<sup>-3</sup> torr deposition pressure as shown in Fig. 3(a). In AC-CVD there is C1s peak at 284-285 eV with 15 minutes etching with Argon ion, 5.7x10<sup>-1</sup> torr in deposition pressure, but in the 60 minutes Argon ion etching, at 1.8x10<sup>+2</sup> torr deposition pressure, there is another peak at about 286.6 eV which should be from C-OH bonding during deposition because of higher deposition pressure as shown in Fig. 3(b).

The laser Raman microprobe spectrometer, renishaw Model Ramascope 2000, with laser beam from the laser diode set at 782 nm wavelength was used to investigate the chemical structure of thin films or crystallites through an optical with 500x magnification for the most of all samples.

The impurity in thin film was not detected by EDS technique in SEM, except oxygen and gold which should come from gold coating for SEM experiment.

### 4. Conclusions

The AC-CVD method appears to be promising for diamond thin film production in more effective than HF-CVD in epitaxial growth.

### Acknowledgment

The authors wish to thank the Thailand Research Fund (TRF) and Khon Kaen University for financial support of this research under contract no.RSA/19/2543.We thank Dr. Yoichiro Sato so much from NIRIM, Tsukuba, Japan for supporting the synthetic diamond plates for standard calibration in characterization. The Metallurgy

Department, Faculty of Engineering, Chulalongkorn University, Bangkok, Thailand is also thanked for helping with the XPS characterization.

### References

- [1] J.C. Williams, Status and applications of diamond and diamond-like materials: emerging technology, National Research Council Rep.NMAB-445, 30 April 1990, (National Materials Advisory Board, Committee on Superhard Materials) National Academic Press.
- [2] H Vora and T.J. Moravec, J. Appl. Phys., 52 (1981)6151.
- [3] M. Kitabatake and K. Wasa, J. Vac. Sci. Technol., A 6(1988) 1793.
- [4] H. Koinuma, M. Kawasaki, M. Funabashi, T. Masegawa, K. Kishio, K. Kitazawa and K. Fueki, J. Appl. Phys., 62 (1987) 1524.
- [5] V. Amornkitbamrung and N. Suttisiri, Surface and Coating Technology, 47 (1991) 533.
- [6] V. Amornkitbamrung and N. Suttisiri, Applications of Diamond Films and Related Materials: Third International Conference, 1995, pp.793-796, Editors: A. Feldman, Y. Tzeng, W.A. Yarbrough, M. Yoshikawa, and M.Murakawa.
- [7] T. Ando, H. Haneda, M. Akaishi, Y. Sato and M. Kamo, Diamond Relat. Mater., 5 (1996) 34.
- [8] D.N. Belton and S.J. Schmieg, J. Vac. Sci. Technol. A 8 (1990) 2353.
- [9] P. Reinke, J.E. Klemberg-Sapieha and L. Matinu, J. Appl. Phys. 76 (1994) 5754.
- [10] J. Shirafuji, Y. Sakamoto, A. Furukawa, H.Shigeta and T. Sugino, *Diamond Relat. Mater.*, 4 (1995) 984.
- [11] N. Yokonaga, Y. Katsu, T. Machida, T. Inuzuka, S. Koizumi and K. Suzuki, Diamond Relat. Mater., 5 (1996) 43.
- [12] C. Benndorf, S. Hadenfeldt, W. Luithardt and A. Zhukov, Diamond Relat. Mater., 5 (1996) 784.
- [13] P. Karve, J.P. Pal, S.C. Patil, A.A. Kulkarni, S.M. Kanetkar, N. Parikh, B. Patnaik and S.T. Kshirsagar, *Diamond Relat. Mater.*, 5 (1996) 1527.

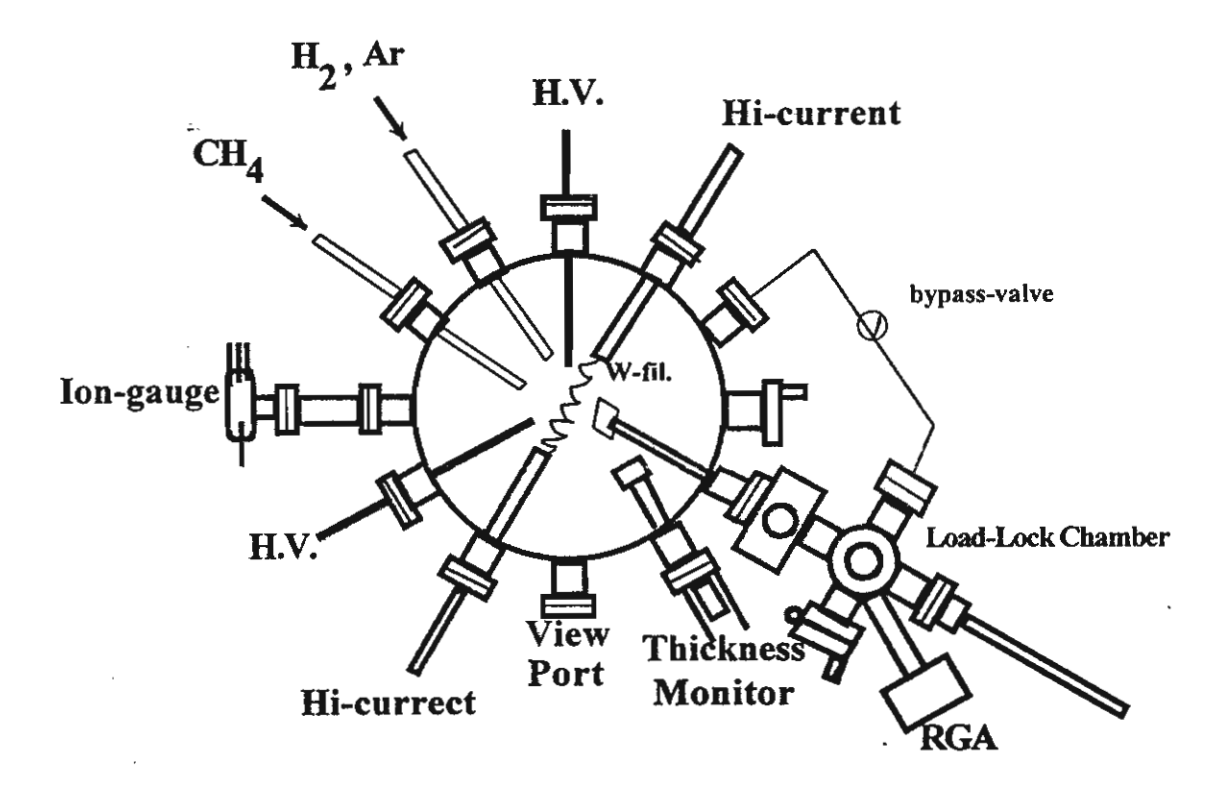
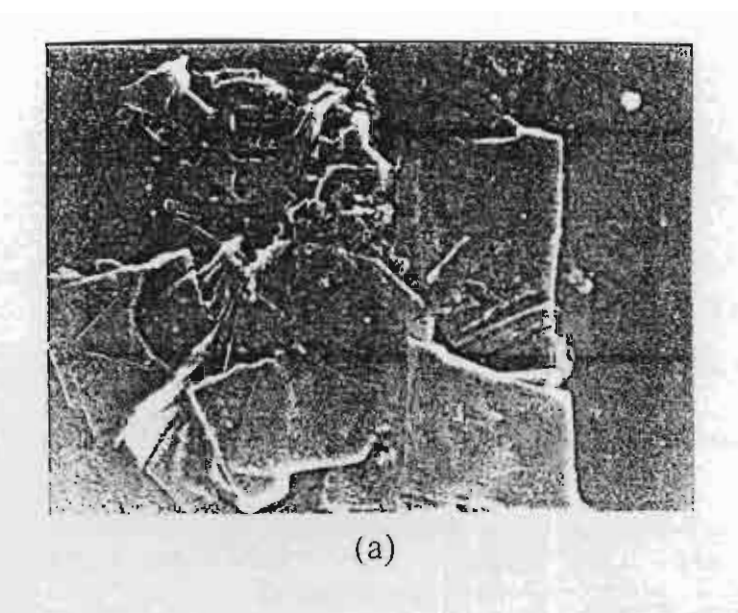


Fig.1 A schematic of the alternating current graphite electrodes (ACGE) sputtering + hot filament (HF) CVD hybrid system; H.V. = high voltage feedthroughs, Hi-current = high current feedthroughs, W-fil. = tungsten filament, RGA = residual gas analyzer.



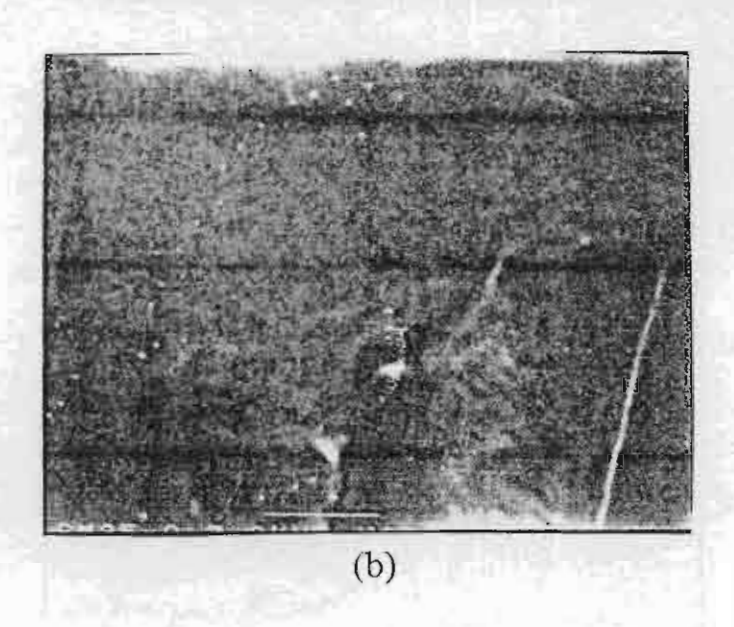


Fig. 2 SEM images (a) from AC-CVD and (b) from HF-CVD processes.

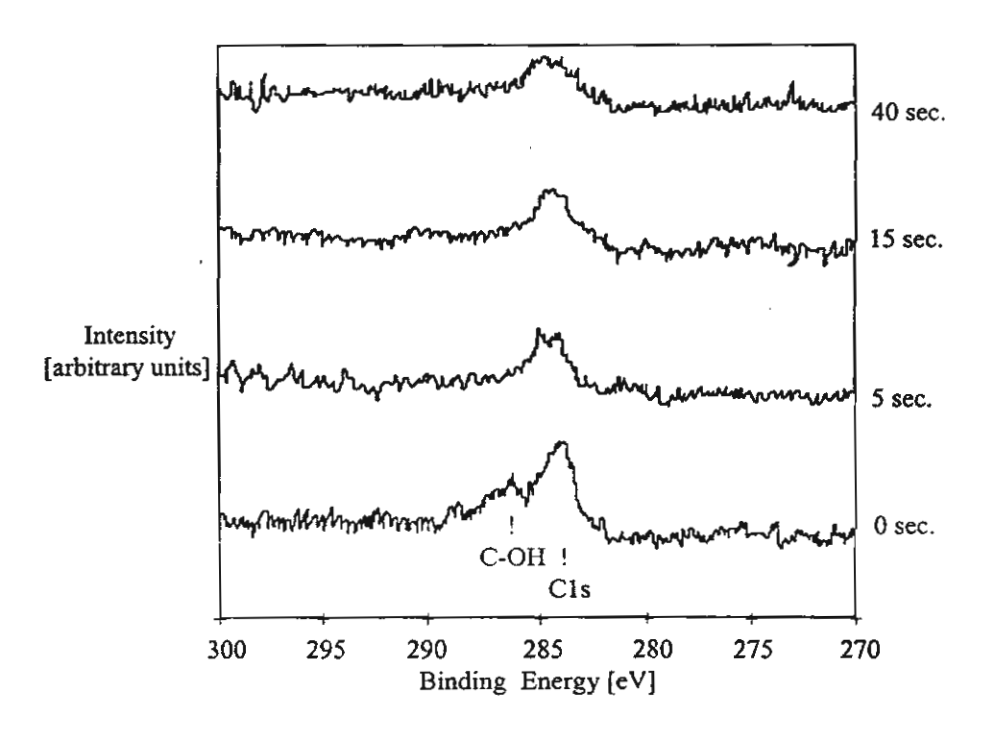


Fig.3 (b) XPS of sm16 from AC-CVD process in 0, 5, 15 and 40 seconds argon ion etching in preparation chamber of XPS setup.

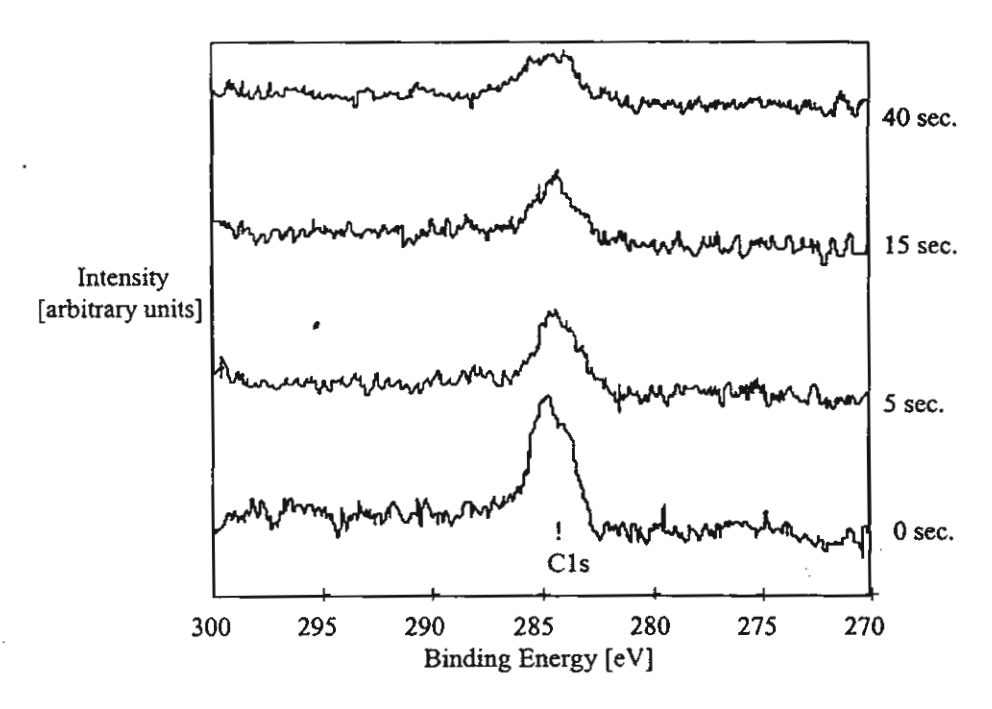


Fig. 3 (a) XPS of sm8 from HF-CVD process in 0, 5, 15, and 40 seconds argon ion etching in preparation chamber of XPS setup.

Table 1 Summary of preparation conditions in this study.

sample no.	base pressure (torr)	surface treatment	deposition technique	deposition time	deposition pressure (torr)
sm6	6.1x10 <sup>-8</sup>	15 min. heat	HF-CVD	5 hours	3.5x10 <sup>-1</sup>
sm14	7.8x10 <sup>-8</sup>	30 min. heat	HF-CVD	5 hours	3.2x10 <sup>-1</sup>
sm12	7.8x10 <sup>-8</sup>	30 min. heat	HF-CVD	5 hours	3.7x10 <sup>-2</sup>
sm5	5.9x10 <sup>-8</sup>	30 min. heat	HF-CVD	5 hours	3.9x10 <sup>-3</sup>
sm8	1.9x10 <sup>-8</sup>	60 min. heat	HF-CVD	5 hours	4.3x10 <sup>-3</sup>
sm9	1.8x10 <sup>-8</sup>	15 min. Ar etch	AC-CVD	5 hours	5.7x10 <sup>-1</sup>
sm13	3.1x10 <sup>-8</sup>	30 min. Ar etch	AC-CVD	5 hours	3.5x10 <sup>-1</sup>
sm15	2.8x10 <sup>-8</sup>	45 min. Ar etch	AC-CVD	5hours	2.2x10 <sup>+2</sup>
sm16	2.1x10 <sup>-8</sup>	60 min. Ar etch	AC-CVD	5 hours	1.8x10 <sup>+2</sup>

Table 2 Comparison XPS results between our work and other work from literature reviews [8-13].

comment	C-O bonding	hydrocarbon bonding	C-C bonding	References
natural diamond (111)	-	-	284.3 eV (1x1)	Shirafuji (1995) refer Pate (1986)
natural diamond			284.8 eV	Shirafuji (1995)
(111) anneal 1100 C	-		(2x1)-(2x2)	refer Pate (1986)
CVD diamond	285.5-286.8 eV	285.3 eV adsorbed hydrocarbon	284.8 eV	D.N. Belton (1990)
CVD diamond	-	-	284.6 eV	Reinke (1994)
CVD diamond anneal + O2 plasma	289.9 eV	288.7 eV, C-OH	287.2 eV	Shirafuji (1995)
CVD diamond anneal	288.9 eV	287.8 eV , C-OH	286.4 eV	Shirafuji (1995)
CVD diamond anneal + Ar etch	288.2 eV	287.0 eV , C-OH	285.4 eV	Shirafuji (1995)
CVD diamond	-	-	284.4 eV	N. Yokonaka (1996)
CVD diamond	288.1 eV	-	284.6 eV	Karve (1996)
CVD diamond	287.3 eV	-	284.2 eV	C. Benndorf(1996)
CVD diamond		286.8 eV	284-285 eV	present work
	-	AC-CVD	AC-CVD, HF -CVD	
synthetic diamond (100)	288 eV before Ar etch	-	284-285 eV after Ar etch	present work

### Session P2.05: Diamond-Like Carbon

of
2 di
ted of
e
using nd Rio



# 8th International Conference

# **New Diamond Science and Technology**

2002

Sunday 21st to Friday 26th July 2002

The University of Melbourne Australia

### P2.05.1

# Surface and quality modification of diamond-like carbon films by CO2 laser heating assisted hot filament chemical vapor deposition

### V. Amornkitbamrung and Ong-On Topon

Department of Physics, Faculty of Science, Khon Kaen University, Khon Kaen 40002, Thailand

The infrared CO2 laser was used for regional heating to study the heat effect on HF-CVD of DLC formation on Si(100) face substrates. The micro-Raman spectrometer and scanning electron microscope were used for characterization of the chemical bonding types and surface morphology. The silicon substrate was loaded into the load-lock system and manually transferred into the ultra high vacuum chamber at a pressure of 10-8 mbar, evacuated by means of combined

titanium sublimation and turbomolecular pump for keeping the silicon surface clean before the deposition process was started. The tungsten filament temperature was about 1850-1950 o C, detected by optical pyrometer. The substrate surface temperature was about 450-500 o C, detected by the chromel-alumel thermocouple. A CO2 laser beam, 2 mm in diameter, continuous wave, was used to heat the substrate for a further 20 minutes. The power of laser was varied by biasing the CO2 laser tube at three different input currents, 6, 7, and 8 mA which raised the temperature of the substrate locally by 25, 45 and 55 0 C respectively. At the medium laser power, the central

laser beam region had a broad Raman peak centered at 1438 cm -1 which had higher intensity than D-peak(1365cm-1) and G-peak(1720cm-1) at the outer region. It can be concluded that this region had good quality DLC. This moderate high frequency peak corresponds to the four-fold rotation symmetry atoms in the amorphous carbon network from the tight-binding molecular dynamic simulation of C.Z. Wang and K.M. Ho1. The SiC Raman sharp peak at 765 cm-1 was observed. This should be a phase at the interface between DLC film and Si substrate. We observed this interface region in the cross-sectional SEM image. In this Raman spectrograph a small peak, about 1080 cm-1 was observed, which may be the nanocrystalline diamond phase which corresponds to some nano-DLC particles observed by SEM.

1. C.Z. Wang and K.M. Ho, Structure, Dynamics, and Electronic Properties of Diamondlike Amorphous Carbon. Phys. Rev. Lett.,71(1993)1184.

# Surface and quality modification of diamond-like carbon films by CO<sub>2</sub> laser heating assisted hot filament chemical vapor deposition



V. Amornkitbamrung and Ong-On Topon
Department of Physics, Faculty of Science, Khon Kaen University,
Khon Kaen 40002, Thailand

An infrared CO<sub>2</sub> laser was used for regional heating to study the heating effect on HF-CVD of DLC formation on Si(100) face substrates. The micro-Raman spectrometer and scanning electron microscope were used for characterization of the chemical bonding types and surface morphology. The silicon substrate was loaded into the load-lock system and manually transferred into the ultra high vacuum chamber at a pressure of 10<sup>-8</sup> mbar, evacuated by means of combined titanium sublimation pump (TSP) and turbomolecular pump (Fig.1) for keeping the silicon surface clean before the deposition process was started. The tungsten filament temperature was about 1850-1950 °C, detected by optical pyrometer. The substrate surface temperature was about 450-500 °C, detected by chromel-alumei thermocouple (TC). A CO<sub>2</sub> laser beam, 2 mm in diameter, continuous wave, was used to heat the substrate for a further 20 minutes. Ultrapure H<sub>2</sub> was flowed into the chamber with a flow rate about 200-215 sccm, followed by flowing CH<sub>4</sub> gas with flow rate about 0.40-0.50 sccm. The power of the laser was varied by biasing the CO<sub>2</sub> laser tube at three different input currents, 6, 7 and 8 mA which raised the temperature on the substrate locally by 25, 45 and 55 °C respectively. These raising temperatures were calculated by the heat conduction equation.

$$\frac{\partial T}{\partial t} = k \nabla^2 T$$

Where k is the thermal conductivity and T denotes the temporal and spatial distribution of temperature. The deposition conditions were 5 hours and 21-25 mbar of pressure.

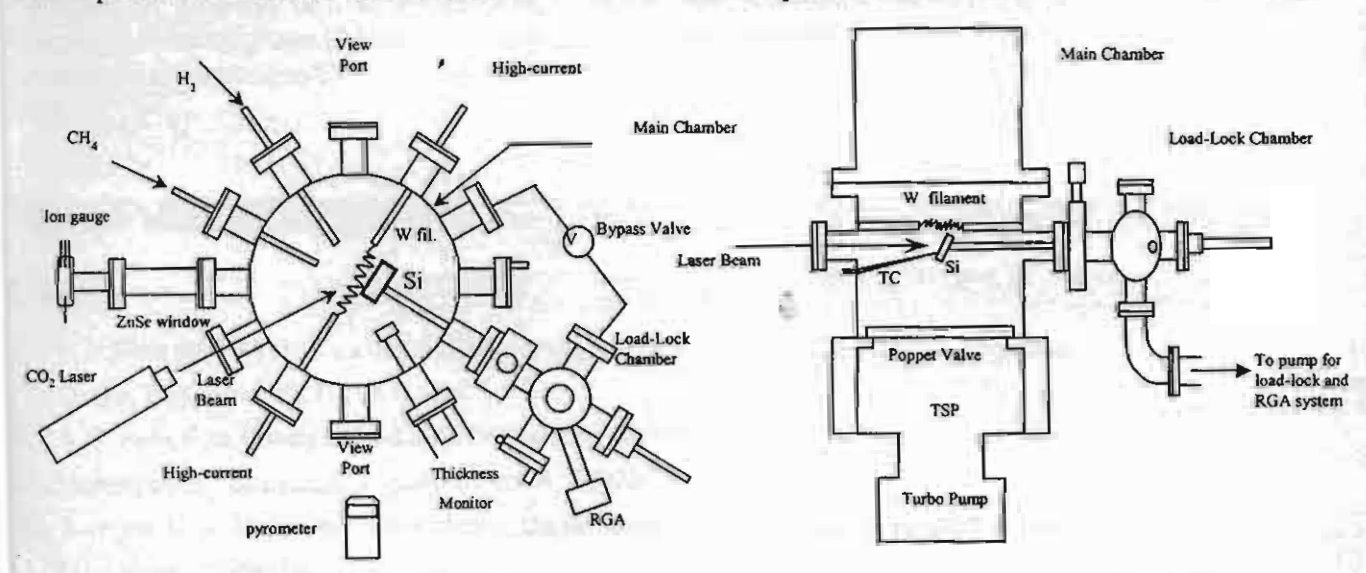


Fig. 1. Plane and sideview diagram of CO<sub>2</sub> laser heating assisted HF-CVD system.

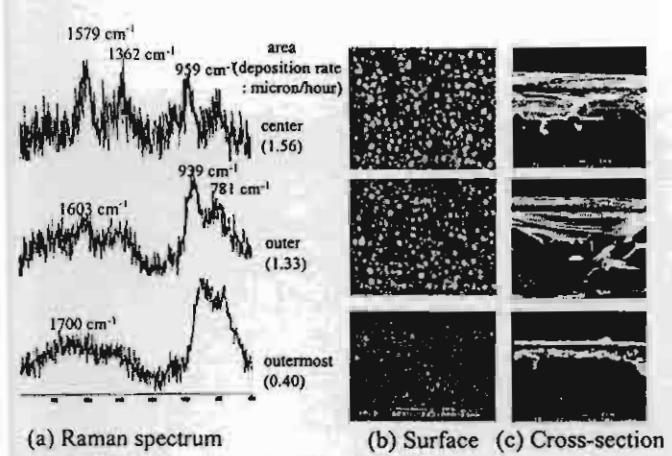


Fig. 2 (a) Raman spectrum (b) surface morphology and (c) cross-section of the low-power laser film has particle size 0.12 micron

### Results

The Raman spectrographs, SEM pictures of surface and cross-section in these deposition conditions are shown in Fig. 2, 3 and 4. For medium laser power, at the central laser beam region a broad Raman peak centered at 1438 cm<sup>-1</sup> was detected which had more intensity than D-peak(1365cm<sup>-1</sup>) and G-peak(1720cm<sup>-1</sup>) at the outer region. It can be concluded that this region had a good quality of DLC. This moderate high frequency peak corresponds to the four-fold rotation symmetry atom in amorphous carbon network from the tight-binding molecular dynamic simulation of C.Z. Wang and K.M. Ho[1]. The SiC Raman sharp peak at 765 cm-1 observed should be due to a phase at the interface between DLC film and Si substrate. We observed this interface region in the cross-sectional SEM image. In this Raman spectrograph a small peak about 1080 cm-1 was observed. This may be nanocrystalline or amorphous diamond phase [2,3] in cluster which corresponds to some nano-DLC particles observed by SEM.

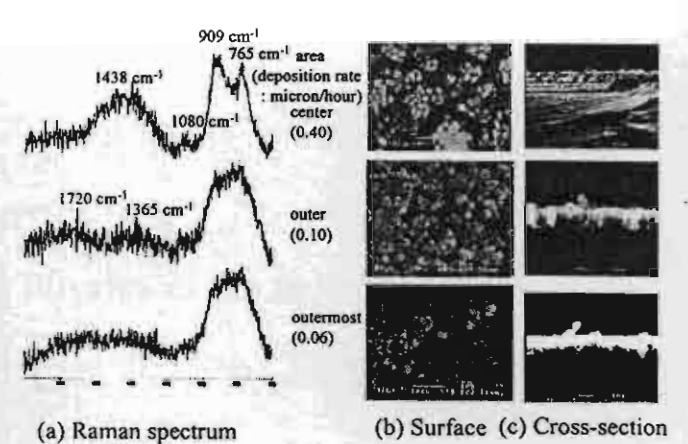


Fig. 3 (a) Raman spectrum (b) surface morphology and (c) cross-section of the medium-power laser film has particle size 0.20 micron

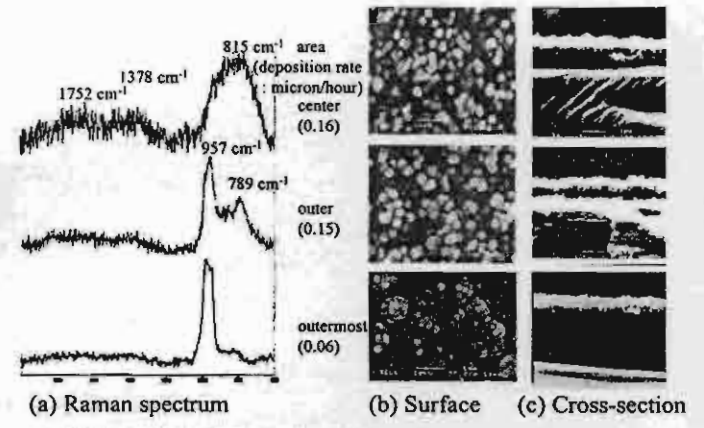


Fig. 4 (a) Raman spectrum (b) surface morphology and (c) cross-section of the high-power laser film has particle size 0.25 micron

### Conclusion

In DLC deposition by laser assisted HFCVD, the temperature had more effect on pure DLC phase and homogenous surface. We observed the most homogenous DLC deposition condition for coating on Si substrate which can be applied for development of solar cell efficiency improvement.

This work was supported by the Thailand Research Fund: contract number RSA/19/2543

### Reference

- C.Z. Wang and K.M. Ho, <u>Structure, Dynamics, and Electronic Properties of Diamondlike Amorphous</u>
   <u>Carbon. Phys. Rev. Lett.</u>, 71 (1993) 1184.
- A. V. Rode, E. G. Gamaly and B. Luther-Davies, <u>Formation of Cluster-assembled Carbon Nano-foam by</u> <u>High-repetition-rate Laser Ablation</u>. Appl. Phys. A, 70(2000) 135.
- S. Prawer, K. W. Nugent and D. N. Jamieson, <u>The Raman Spectrum of Amorphous Diamond</u>. Diamond Relat. Mater., 7(1998) 106.

### Proceedings of the Thai Physics in the next century

December 22-23, 2000 Chulalongkorn University Bangkok THAILAND

### Editors: Virulh Sa-yakanit Chanin Churrahmun

Forum for Theoretical Science (FTS), Department of Physics, Faculty of Science, Chulalongkorn University, Bangkok, THAILAND



Support by:
The National Research Council of Thailand

### TABLE OF CONTENTS

Biological Physics Virulh Sa-yakanit and Piyapol Anubuddhangkura	Page 1-18
Generalized Calculation of and Interferometer with Signal Processing Applications S. Suchat, T. Charnuwong and P.P. Yupapin	19-26
Effect of Firing Temperature on Phase Transformation and Microstructure Development in Lead Titanate Ceramics  A. Udomporn, S. Ananta and T. Tunkasiri	27-31
Real Time Physics: Motion Studies Tharest Thanakitivirun and David Wheeler	32-39
Algebraic description of the core-plus-alpha-particle cluster states of the <sup>44</sup> Ti nucleus A. Intasorn, J. Cseh, G. Levai and K. Kato	40-45
Initial Diamond Growth Study of the Chemical Vapour  Deposition Process by CO <sub>2</sub> Laser Heating  Vittaya Amornkitbamrung, Ong-On Topan and Wirat Jarernboon	46-51
Interband Transition Studies on Er- \delta doped InP by Photeurrent Spectroscopy Wisanu Pecharapa and Jiti Nukeaw	52-59
Harmonics By DSP: Quick, Accurate and Reproducible Tharest Thanakitivirun, Vittaya Tipsuwanporn and David Wheeler	60-64
Microstructure of BaTi <sub>4</sub> O <sub>9</sub> ' Prepared by Solid State Reaction Method S. Tangjuank, T. Tunkasiri and S. Ananta	65-71
Characteristic of Polymer Membranse: The Effect of DC Voltage on Diffusion Potentials Pikul Wanichapichart, Wanida Sumethakulawat and Amnuoy Keawpil	72-82 5000n
A Coherence Length Shortening of Long Coherence Laser Beam For Interferometric Use P.P. Yupapin	83-91

Appendix

Proceeding of the Thai Physics in the next century, December 22-23, 2000

# Initial Diamond Growth Study of the Chemical Vapour Deposition Process by CO<sub>2</sub> Laser Heating

Vittaya Amornkitbamrung, Ong-On Topon and Wirat Jarernboon.

Department of Physics, Faculty of Science, Khon Kaen University, Khon Kaen 40002, Thailand

Key words: CO2 laser, hot filament, XRD

### Abstract

Initial diamond growth was studied in a UHV chamber at an ultimate pressure of 10°8 Torr by online monitoring of the gas mixture composition with a quadrupole mass spectrometer during the deposition process. The CH<sub>4</sub>-H<sub>2</sub> mixed gas, hot filament chemical vapour deposition method was used in diamond thin film deposition on silicon (100) substrate in a temperature range of 1,700-1,800 °C and 20 millibar deposited pressure. A CO<sub>2</sub> laser beam was used to raise the temperature locally on the substrate surface. The crystal shape and surface morphology were observed by optical microscope. An X-ray diffractometer was used to study the stress over the sample by observing the (311) silicon diffracted peak shift at some incident X-ray beam glancing angles. The stress distribution on the irradiated sample is more homogeneous than the normal sample.

### 1. Introduction

Diamond is a material which has unique properties better than other materials in many ways such as optical transparency from X-rays to infrared radiation, high thermal conductivity five times that of copper, inert for chemical agents, extreme hardness and can withstand radioactivity. It is a good insulator, but it can be doped to become a semiconductor for device applications in an aggressive corrosion, high temperature and high radiation environment.

A laser was used to assist chemical vapour deposition for improved homogeneity, adhesion to substrate, surface smoothness, and electrical properties [1]-[8].

In this research, a CO<sub>2</sub> laser was used to assist the hot filament chemical vapour deposition (HF-CVD) of diamond thin film on silicon (100) at a low pressure, 10-30 mbar. The optical microscope and X-ray diffractometer were used to observe surface morphology and stress distribution respectively.

### 2. Experimental Procedure

A Si(100) wafer, p-type, 1 inch in diameter and 0.30 mm in thickness, was sectioned into specimens 10 mm x 10 mm and cleaned with acetone and methanol in an ultrasonic cleaner for 1 hour in each solvent, rinsed with deionized water and dried with dry nitrogen for a few minutes. The silicon substrate was loaded into the load-lock

system and manually transferred into the ultra high vacuum chamber at a pressure of 10<sup>-8</sup> Torr, evacuated by means of combined titanium sublimation and turbomolecular pump, as show in the photograph of the system in Fig.1. The silicon substrate was about 1-2 mm from a tungsten filament circular coil and the substrate was " in situ " thermally cleaned with thin hot filament for 1 hour. The filament temperature was about 1,600-1,800°C, detected by optical pyrometer. The substrate surface temperature was about 500-600 °C, detected by the chromel-alumel thermocouple. A CO<sub>2</sub> laser beam, 1 mm in diameter, continuous wave, was used to heat the substrate for a further 20 minutes. Ultra pure H<sub>2</sub> gas was flowed into the chamber with flow rate about 180-200 sccm, followed by flowing CH<sub>4</sub> gas with flow rate about 0.35-0.50 sccm. The conditions for thin film deposition on seven Si (100) samples are summarized in Table 1.

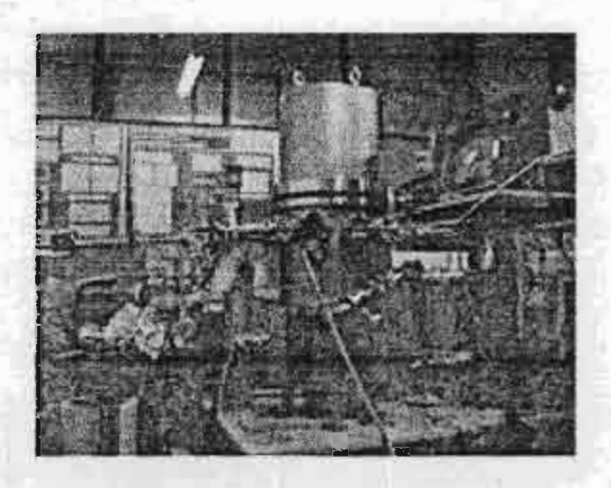
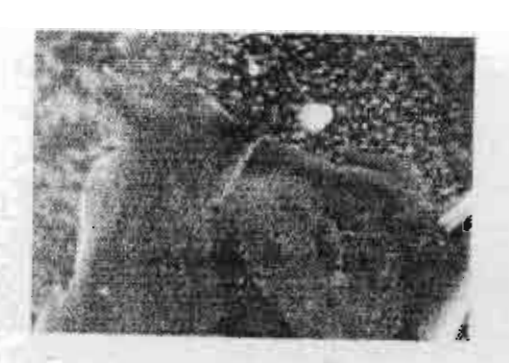


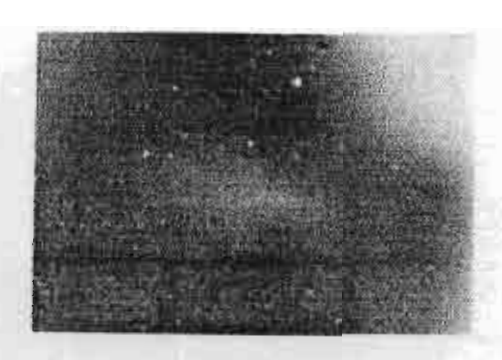
Fig. 1 The photograph of the system.

Table 1 Summary of preparation conditions.

Sample	Pressure (mbar)	T <sub>filament</sub>	T <sub>substrate</sub>	H <sub>2</sub> rate (sccm)	CH <sub>4</sub> rate (sccm)	Deposition time	CO <sub>2</sub> laser time
DIL01	30	1,650	400	180	0.35	3 hr	3 hr
DIL02	10	1,675	555	210	0.45	4 hr	2 hr
DIL03	25	1,700	555	190	0.40	4 hr 40 min	4 hr
DIL04	20	1,600	560	190	0.50	10 hr	10 hr
DIL05	20	1,800	580	180	0.40	10 hr.	All Paris
DIL06	25	1,800	600	180	0.45	20 hr	
DIL07	20	1,850	570	180	0.50	20 hr	None

The surface morphology of the deposited diamond was observed by optical microscope, 100x and 400x magnifications. Results are shown in Fig.2





(a) (b)

ig. 2. The surface morphology of the deposited diamond was of

Fig. 2 The surface morphology of the deposited diamond was observed by optical microscope (a) 400x of DIL01 (b) 100x of DIL02

The deposited thin film was structurally analyzed by means of a parallel beam X-ray diffractometer, using a power of 40 kV, 35 mA from Cu anode X-ray tube, with a divergence slit width of 1/6°. The results were analyzed by comparing peaks with ASTM standard values as shown in Table 2.

Table 2 Summary of d-spacings, observed values and ASTM standard.

Material (hkl)	ASTM standard o (A)	DIL01	DIL02 ° (A)	DIL03	DIL04 ° (A)	DIL05 ° (A)	DIL06 (A)	DIL07 (A)
SiO <sub>2</sub> (101)	3.343	-	-	-	3.1246			
β-SiC(310)	2.510	2.5225				-	-	-
SiC(101)	2.360	-	100		2.3562	2.3394	2.3733	2.3480
α-SiC(018)	2.320	-		-	2.3562	2.3394	2.3733	2.3480
SiC(018)	2.317	-	3,414	2.3070	-			-
SiO <sub>2</sub> (102)	2.882	-	2.7520		-	-	-	-
SiO <sub>2</sub> (111)	2.237		2.2384		-	-		-
α-SiC(01,13)	2.230	2:2355	1	fi -	C	-		-
SiC(104)	2.179	-	2.1655	- 1	2.1704		-	
β-SiC(200)	2.170	-			2.1704	~	-	-
Diamond(111)	2.060	2.0310	2.0339	2.0380	2.0376	2.0376	2.0376	2.0292
Graphite(111)	2.039	2.0310	2.0339	2.0380	2.0376	2.0376	2.0376	2.0292
α-SiC(01,41)	2.030	2.0310	2.0339	2.0380	2.0376	2.0376	2.0376	2.0292
Graphite(101)	2.027	2.0310	20.339	2.0380	2.0376	2.0376	2.0376	2.0292
α-SiC(01,43)	1.980		1.9180	-	-	-		-
β-SiC(220)	1.540	_ 0		1.5490	-	-	- 1	H 2
β-SiC(222)	1.260		-		1.2240	·		1.2229
Diamond(220)	1.261	1.2511	-	-	1.2240	-	-	1.2229
Graphite(110)	1.228		-	-	1.2240			1.2229
SiO <sub>2</sub> (310)	1.180	-	-	1.1610			-	1.2229
Diamond(311)	1.075			1.0540		-	1.0126	1 - 2
Graphite(201)	1.050	-	-		-	-	1.0126	
SiO <sub>2</sub> (223)	1.014			-			1.0126	

Table 2	Summary	of d-spacings,	observed	values and ASTM	standard.(cont.)
	,				,

Material (hkl)	ASTM	DIL01	DIL02	DIL03	DIL04	DIL05	DIL06	DIL07
	standard	c	0	0	0	o	٥	o
	o	(A)	(A)	(A)	(A)	(A)	(A)	(A)
	(A)							
β-SiC(311)	1.000	<b>-</b> _	-	-	-		1.0126	-
Graphite(203)	0.9601	-	-	-	0.9299	0.9293	-	-
SiO <sub>2</sub> (410)	0.9280	-	0.9293	-	0.9299	0.9293	-	-
Diamond(400)	0.8916	-	•	0.8902	0.9299	0.9293	-	•
Graphite(008)	0.8774	-	0.8675	-	-	-	-	•
Graphite(116)	0.8256		-	-	-	-	0.8200	•
Diamond(331)	0.8182	-	-	-	-	-	0.8200	-

Stress and strain distribution were investigated from the silicon diffraction peak (311) using an incident X-ray beam at fixed small angles with two different sample orientations, which are called normal and parallel to the X-ray beam as shown in Fig.3. By considering the equation which governs stress and strain by the peak shift plot [9] as

$$\frac{d_{\psi} - d_0}{d_0} = \frac{1 + \upsilon}{E} \sigma \sin^2 \psi$$

where  $\psi$  = incident X-ray beam angle with respect to the sample surface,  $d_{\psi}$  = d-spacing calculated from the peak which corresponds to the incident X-ray beam angles with respect to sample surface,  $\upsilon$  = Poisson's ratio = 0.28 for silicon, E = Young's modulus = 1.67 x 10<sup>10</sup> Pa for silicon. By plotting the graph using the relation between  $\frac{d_{\psi} - d_{0}}{d_{0}}$  and  $\sin^{2} \psi$ , we obtain a slope, which is equal to  $\frac{1 + \upsilon}{E} \sigma$ . By substitution  $\upsilon$ 

and E for silicon we obtain a stress  $\sigma$ . A summary of the stress of six samples with two orientations is shown in Table 3.

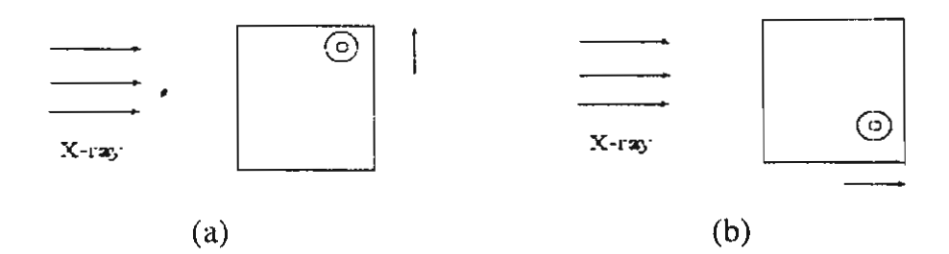


Fig. 3 An incident X-ray beam at fixed small angles with two different sample orientations,

which are called (a) normal to the X-ray beam and (b) parallel to the X-ray beam for investigation of the silicon diffraction peak (311).

**Table 3** A summary of the stress from X-ray diffraction peak shift plot.

Samples	Stress (GPa)	Note
DIL02	3,310	Normal to the X-ray beam
	3,419	Parallel to the X-ray beam
DIL03	3,424	Normal to the X-ray beam
	3,465	Parallel to the X-ray beam
DIL04	3,422	Normal to the X-ray beam
	3,402	Parallel to the X-ray beam
DIL05	3,388.	Normal to the X-ray beam
	3,976	Parallel to the X-ray beam
DIL06	3,437	Normal to the X-ray beam
	3,246	Parallel to the X-ray beam
DIL07	3,364	Normal to the X-ray beam-
	3,439	Parallel to the X-ray beam

### 3. Results and Discussion

From the optical microscopic image, 400x in Fig. 2(a), sample no. DIL01, different grain sizes are seen at the upper right corner of the image which is near laser beam position. There are different crystallites which are parallel as indicated by the heteroepitaxial characteristic of crystallites on the substrate. Some big crystallites show the upper part of octahedral crystals. In the optical microscopic image, 100x in fig. 2 (b), sample no.DIL02 showed different colors, which should come from refractive dispersion patterns from incident white light on the sample because of thin film thickness being gradually different from laser position at the upper right corner of the image.

From the X-ray diffraction analyzed data in Table 2, there are some diffracted peaks which are comparable with ASTM standard  $\beta$ -SiC and diamond peaks, such as  $\beta$ -SiC(220),  $\beta$ -SiC(222), diamond(311) and diamond(400). These peaks have d-spacing values less than ASTM standard values, which occurred because of stress and strain on the silicon substrate. These effects come from lattice mismatching between the thin film and substrate materials. The stress distribution is modified from an elliptical area to a circular area as shown in Table 3 for sample nos. DIL02, DIL03, DIL04 and DIL07, especially in DIL04 which was irradiated with CO2 laser for a longer time of 10 hr.

ŧï.

### 4. Conclusion

It can be concluded that the  $CO_2$  laser heating on substrate surface can modify the early stage of diamond deposition on silicon(100) substrate. The buffer layer phase,  $\beta$ -SiC crystalline is also qualitatively improved and this makes the diamond layer more perfect in the crystalline structure. This method may improve the quality of heteroepitaxial diamond thin films on silicon, and can be used in electronic applications.

### 5. Acknowledgments

This research was funded by the Local Graduate Scholarship of the National Science Technology and Development Agency (NSTDA). It was also funded by the Thailand Research Fund (TRF) under contract no. RSA/19/2543 and Khon Kaen University. We are indebted to Assistant Professor Pipat Chokesuwattanaskula for giving us a CO<sub>2</sub> laser for this research.

### Reference

- 1. Fujimori Susumu, Kasai Toshio, Inamura Takahiro. Carbon film formation by laser evaporation and ion beam sputtering. *Thin Solid Films* 1982; 92: 71-80.
- Tyndall George W, Hacker Nigel P. KrF\* laser-induced chemical vapor deposition of diamond. Diamond, Silicon Carbide and Related Wide Bandgap Semiconductors, Symposium held November 27-December 1, 1989, Boston, Massachusetts, U.S.A. Materials Research Society Symposium Proceeding 1989; 162: 173-178.
- 3. Pehrsson Pehr E, Nelson HH, Celii FG. Investigations of excimer laser effects on CVD diamond growth. Diamond, Silicon Carbide and Related Wide Bandgap Semiconductors, Symposium held November 27-December 1, 1989, Boston, Massachusetts, U.S.A. *Materials Research Society Symposium Proceeding* 1989; 162: 179-184.
- Rengan A, Biunno N, Narayan J. Laser assisted techniques for diamond and diamond-like thin films. Diamond, Silicon Carbide and Related Wide Bandgap Semiconductors, Symposium held November 27-December 1, 1989, Boston, Massachusetts, U.S.A. Materials Research Society Symposium Proceedings 1989; 162: 185-188.
- 5. Metev SM, Ozegowski M, Meteva K, Sepold G, Kononenko TV. Konov VI, Obraztsova ED, Pimeso ED, Pimenov SM, Ralchenko VG, Smolin AA. Laser-assisted ECR-plasma-CVD of a C: H films. *Diamond and Related Materials* 1996.;5: 420-424.
- 6. Johnson SE, Ashfold MNR, Knapper MP, Lade RJ, Rosser KN, Fox NA, Wang WN. Production and characterisation of amorphic diamond films produced by pulsed laser ablation of graphite. *Diamond and Related Materials* 1997;6:569-573.
- 7. Lindstam Mikael, Boman Mats, Carlsson Jan-Otto. Area selective laser chemical vapor deposition of diamond and graphite. *Applied Surface Science* 1997;109/110:462-466.
- 8. Badzian A, Weiss BL, Roy R, Badzian T, Brawl W, Mistry P, Turchan MC. Characterization and electron field emission from diamond coating deposition by multiple laser process. *Diamond and Related Materials* 1998;7:64-69.
- 9. Amornkitbamrung Vittaya. Stress and strain in heteroepitaxial diamond thin film on Si(100) observed by X-ray diffraction and X-ray diffraction topography. *Diamond Films and Technology* 1998; 8(3):138.

วกสารประกอบการประชุม การประชุมวิชา**การทาวด้าน** 

# วิทยาศาสตร์และเทคโนโลยีวัสถุ แห่วประเทศไทย ครั้วที่

The Second Thailand Materials Science and Technology Conference : Materials Science and Technology for a Sustainable Development of Thailand

6 – 7 สิงหาคม 2545

อาคารสารนิเทศ 50 ปี มหาวิทยาลัยเกษตรศาสตร



ำกไดย ผูนยกกไนโลยีโดกะและวัสถุแก่งชาติ (เอ็มแาย)



# ORAL PRESENTATIONS

•							
วส	ดข	าาเ	ากเ	าร	แา	พท	Ł

B1	The Design of Custom Biocompatible Implants for Skull Reconstruction Surgery by Means of	
	Reverse Engineering and Rapid Prototyping	
	P. Oris, K. Sitthiseripratip, J. Suwanprateeb and J. V. Sloten	
B2	Finite Element Analysis of an Orthopaedic Device Inserted in the Proximal Femur :	
	The Value of Coloured RP Models for Concept Modelling	;
	K. Sitthiseripratip, P. Oris, B. Mahaisavariya, J. Suwanprateeb, H. V. Oosterwyck, J. V. Sloten and E	. Bohez
В3	เครื่องย้ายขึ้นงานสลับร้อนเย็นอัตโนมัติสำหรับงานทคสอบวัสคุทางทันตกรรม	6
	อนุพงศ์ สรงประภา, สุรศักดิ์ บุญกล้า และ ประจักษ์ ทองจันทร์	
B4	การกำซาบฮิ้นส่วนทางชีวภาพด้วยสารพลาสติก	ç
	อุทัย ตันกิตติวัฒน์, เอมอร เจริญสรรพพืช และ พูลพล ผคุงฮัยโชติ	

### เซรามิกส์

C1	A Simple and Inexpensive Technique for Low-Temperature Deposition of Nanocrystalline		
	SnO <sub>2</sub> Thin Films	12	
	S. Supothina		
C2	ทั้งสเตนออกไซต์และการประยุกต์ใช้งานเป็นก๊าชเซนเซอร์วัดแอลกอฮอล์	15	
	มานะ ศรียุทธศักดิ์ และ สิทธิสุนทร สุโพธิณะ		
C3	Nitrogen Dioxide Sensing Characteristics of Lead Phthalocyanine in Polypyrrole	18	
	R. Tongpool and S. Yoriya *		
C4	Effect of Maisture Contents on Ball Clay Suspensions	21	
	T. Tonthai		
C5	ผลของปริมาณสารช่วยกระจายตัวต่อสมบัติการหล่อแบบชิลิกอนคาร์ไบด์สเลอรี	24	
	กรรณิการ์ เดชรักษา, ผกามาศ แซ่หว่อง และ กุลจิรา สุจิโรจน์		
C6	ผลของขนาดผงฮิลิคอนต่อสมบัติทลังการเผาผนึกขั้นดัน	27	
	กิตติมา ศิลปษา, ไสว ด่านชัยวิจิตร และ กุลจิรา สุจิโรจน์		
C7	Utilization of Rice Husk as Silica Source for Mesoporous Molecular Sieve Synthesis	30	
	N. Grisdanurak, W. Suriyakrai, J. Wittayakun and S. Chiarakorn		
C8	Alumina/Silicon Carbide Nanocomposite Ceramic Coatings via Plasma Spraying Technology	33	
	S. Jiansirisomboon , S. G. Roberts and P. S. Grant		
C9	Crack Healing and Strength Recovery in Thermally-Shocked Alumina-SiC Nanocomposite	38	
	S. Maensiri and S.Roberts		
C10	Effect of Polarization on the Fracture Toughness of BaTiO <sub>3</sub> -Al <sub>2</sub> O <sub>3</sub> Composites	39	
	S. Rattanachan, Y. Miyashita and Y. Mutoh	1	

C11	การนำวัสคุเทลือทั้งจากขบวนการหลอมเทล็กมาใช้ในงานคอนกรีต	42
	อิทธิพร ศิริสวัสดิ์, ซูศักดิ์ ภู่เจริญวณิชย์ และ นวนิด ร่วมเจริญกิจ	
C12_	<u>การเคลือบวัสดุด้วยคาร์บุอนคล้ายเพชรด้วยวิธีสปัตเตอริงจากไฟฟ้ากระแสสลับ</u>	45
	วิทยา อมรกิจบำรุง, องค์อร ดอพล, วิรัตน์ เจริญบุญ, สุมินทร์ญา ที่ทา และ รวิพร บุญศิริ	
C13	Solid State MAS NMR for Phase Identification in Glass-Ceramic Materials	48
	A. Niyompan and D. Holland	
C14	Ferroelectric Bismuth Germanate (Bi GeO <sub>5</sub> ) Glass-Ceramics	50
	K. Pengpat and D. Holland	
การ	ออกแบบและเครื่องจักรกล	
D1	Analysis of Crack Propagation in Metals by Adaptive Finite Elements	53
	S. Phongthanapanich, P. Bhandhubanyong and P. Dechaumphai	
D2	Effects of Thin Sealant-Like Adhesive Layer on Countersunk Riveted Lap Joint	56
	C. Dechwayukul, T. Fongsamootr, N. Kamnerdtong, C. A. Rubin and G. T. Hahn	
D3	การพัฒนาฐานการเคลื่อนไหวขนาดย่อส่วนของเครื่องจำลองการขับรถยนต์ =	59
	สันติภาพ เชิดซูศิลป์, ซัยวัฒน์ โพธิ์ปริสุทธิ์ และ สุวัฒน์ กุลธนปรีตา	
04	การจำลองกระบวนการลากขึ้นรูปโลทะแผ่นด้วยระเบียบวิธีไฟในต์เอลีเมนต์	62
	ธนสาร อินทรกำธรชัย และ วิโรจน์  ซ่วยซู	
D5	การผลิตฮิ้นงานตัดเที่ยงตรงสูงที่ไม่มีส่วนโค้งมนและรอยฉึกฮาดโดยกรรมวิธีผสมระหว่างการตัดและการเฮฟวิ้ง	66
	สุรพงษ์ ฮัยรัตน์ธรรม, พงศ์พันธ์ แก้วตาทิพย์ และ วารุณี เปรมานนท์	
D6	การศึกษาการลดครึบบนขอบของขึ้นงานตัดโดยกรรมวิธีการกดตัดและดันกลับ	69
	นทีซัย ผัสดี, พงศ์พันธ์ แก้วตาทิพย์ และ วารุณี เปรมานนท์	
D7	การออกแบบและสร้างอุปกรณ์ RCC	72
	ธรรมรัศน์ กิตติพงษ์พัฒนา	
D8	การออกแบบและสร้างอุปกรณ์การวัดการรั่วไหลของเส้นแรงแม่เหล็กเพื่อตรวจสอบรอยบกพร่องแบบ	
	เฉพาะที่ของสายเคเบิล	76
	เชิดพงษ์ จอมเดช, อาษา ประทีปเสน และ วชิระ มีทอง	
D9	การจำลองการขึ้นรูปถั่วยทรงกระบอกด้วยวิธีโฟในต์เอลิเมนต์ แบบไตนามิค เอ็คพลิซิท / ยึตหยุ่น-พลาสติก	79
	ดิลก ศรีประโพ และ จุลศิริ ศรีงามผ่อง	
ໂພລີ	้เมอร์	
P1	เจา เลย มี การเตรียมถุงมือชนิดไร้แป้งโดยการเคลืองด้วยอะคริลิกพอลีเมอร์ผสมกับกราฟต์โคพอลิเมอร์ฮองน้ำยางธรรมชาติ	
71	การเตรยมถุงมออนต์เรณบงเตยการเคลยบตรยอะครลกพอสเมยรมสมุกบกราหต์เคพยสเมยรอยงนะเยางธรรมอาต โปรตีนต่ำกับเมทิลเมทาครีเลท	00
	เจริญ นาคะสรรค์, มัสวานี นราธิฮาติ และ อาซีฮัน แกสมาน	83
P2		86
rz	Crystallization Behavior of Highly-Purified Natural Rubber	86
D2	J. Ruangdech, S. Kawahara and Y. Isono	
P3	Controlled Photodegradation of Natural Rubber Glove by Encapsulated Benzophenone	00
	and 2,6-Di-t-Butyl-p-Cresol Toluene	88
D/I	S. Riyajan, K. Kanyawararak, T. Likhitlaksanakul, J. Sakdapipanich and Y. Tanaka	04
P4	Effect of Hot Plate and Part Geometry on Joint Quality of Hot Plate Welding	91
DE	B. Poopat อิทธิพลของลีค่ออัตราการให้ความร้อนในกระบวนการเชื่อม TTIR	24
P5		94
DC	โชคซัย สิงหธรรม, ณรงค์ฤทธิ์ สมบัติสมภพ และ บวรโชค ผู้พัฒน์	
P6	Mathematical Modeling of Microencapsulation by Interfacial Polycondensation	97
	A. Pathomsakul	

### การเคลือบวัสดุด้วยคาร์บอนคล้ายเพชรด้วยวิธีสปัตเตอริงจากไฟฟ้ากระแสสลับ Diamond-like Carbon Coating on Materials by Alternating Current Sputtering

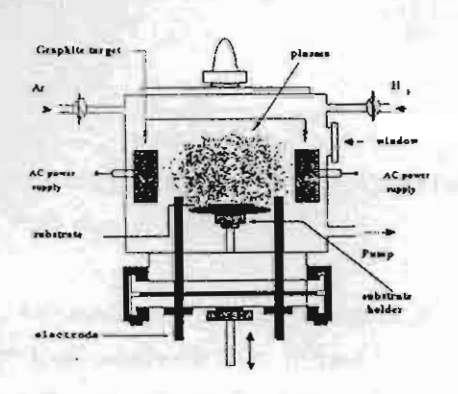
วิทยา อมรกิจบำรุง , องค์อร ตอพล , วิรัตน์ เจริญบุญ , สุมินทร์ญา ที่ทา , รวิพร บุญศิริ ภาควิชาฟิสิกส์ คณะวิทยาศาสตร์ มหาวิทยาลัยขอนแก่น อ.เมือง จ.ขอนแก่น 40002 โทรศัพท์ (043) 242333 - 9 ต่อ 2248 , โทรสาร (043) 244416 , e-mail : vittaya@kku1.kku.ac.th

### บทคัดย่อ

ได้ทำการเคลือบวัสดุด้วยฟิล์มคาร์บอนคล้ายเพชงด้วยวิธีสปัต
เตอริงจากไฟฟ้ากระแสสลับบนเซลล์แสงอาทิตย์เพื่อเพิ่มประสิทธิภาพ
และเคลือบดอกสว่านเพื่อเพิ่มความคงทนในการใช้งาน คาร์บอนคล้าย
เพชรถูกเตรียมที่ความดัน 70-200 มิลลิทอร์ อุณหภูมิของวัสดุฐานรอง
ขณะเตรียมประมาณ 100 องศาเซลเซียส พบว่าการเคลือบคาร์บอน
คล้ายเพชรบนเซลล์แสงอาทิตย์ช่วยให้ประสิทธิภาพเพิ่มขึ้นร้อยละ 27.3
จากประสิทธิภาพเดิมและดอกสว่านใช้เวลาในการเจาะต่อครั้งน้อยลง
Abstract

The diamond-like carbon films were deposited by AC sputtering on solar cell to increase efficiency and on some drills to increase durability. The deposition conditions were 70-200 mTorr in pressure and 100 °C in substrate temperature. The deposition solar cell efficiency was increased between 1,5-27.3%. The deposition drill showed the drilling though a steel plate 5 mm in thickness, it took time less than the normal drill.

คาร์บอนคล้ายเพรรถูกนำมาประยุกต์เพื่อคุณสมบัติที่ดีขึ้นของวัสดุ
ที่ทำการเคลือบ เช่น การเคลือบฟิล์มคาร์บอนคล้ายเพชรบนเซลล์แสง
อาทิตย์เพื่อเพิ่มประสิทธิภาพ การเคลือบบนดอกสว่านเพื่อเพิ่มความคง
ทนและความแจ้ง การเคลือบเลนส์แว่นตาเพื่อป้องกันการขีดข่วน การ
เคลือบหัวอ่านอาร์ดดิสเพื่อป้องกันความเลียหายที่เกิดจากการเสียคสี
ฯลฯ ซึ่งคุณสมบัติเหล่านี้มีประโยชน์อย่างมากในทางอุตสาหกรรม



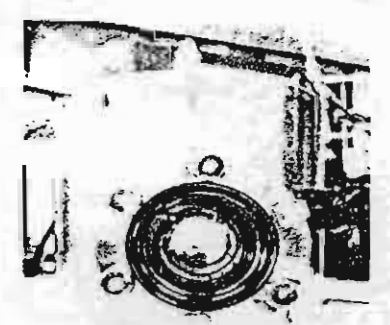
รูปที่ 1 แสดงรายละเอียดระบบสุญญากาศสำหรับวิธีสปัดเตอริงจาก ไฟฟ้ากระแสลลับ

### การทดลอง

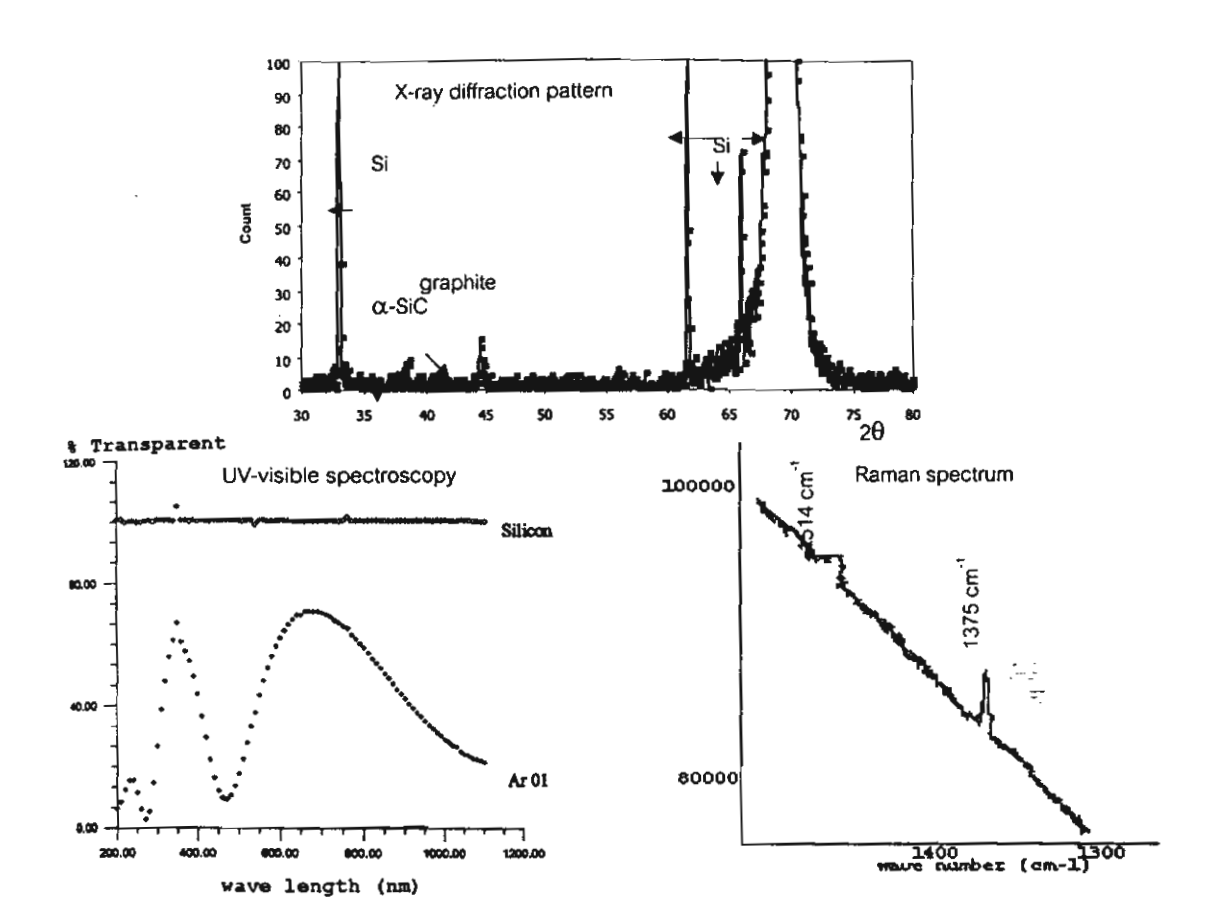
ระบบสุญญากาศแสดงตัง รูปที่ 1และรูปที่ 2 ถูกควบคุมความดัน ด้วยปั้มโรตารี ใช้เป้าแกร์ไฟท์ขนาดเส้นผ่าศูนย์กลาง 4.5 เซนติเมตร 2 เป้าวางห่างกัน 2 เซนติเมตร ให้แรงดันไฟฟ้า 500-1000 โวลด์ ความถี่ 50 เฮิรตซ์ กระแสไฟฟ้า 50 มิลลีแอมแปร์ อุณหภูมิของวัสดุ ฐานรองขณะเตรียมประมาณ 100 องคาเซลเซียส ใช้เวลาในการเตรียม 1-2 ชั่วโมง ในการเตรียมฟิล์มคาร์บอนคล้ายเพชรทำบนวัสดุ 3 ชนิด คือ แผ่นซิลิกอน (100) แผ่นซิลิกอนเซลล์แลงอาทิตย์และคอกสว่าน

คาร์บอนคล้ายเพชรบนวัสดุฐานรองซิลิกอน (100) ขนาด 10×
 มิลลิเมตร<sup>2</sup> ถูกเตรียมที่ความดัน 75 มิลลิทอร์ ในบรรยากาศของ
แก๊สอาร์กอนเป็นเวลา 2 ชั่วโมง ซึ่งเมื่อนำไปตรวจสอบด้วยการเลี้ยว
เบนรังสีเอกซ์พบว่ามี α-SiC เป็นส่วนประกอบของฟิล์มและพบความ
เค้นที่เกิดขึ้นระหว่างคาร์บอนคล้ายเพชรกับวัสดุฐานรองซิลิกอนเป็น
3409 จิกะปาสกาล สเปกตรัมของรามานแสดงพีคที่ 1375 เซนติเมตร์'
ซึ่งเป็นพีคของรามานของเพชรที่เลื่อนไปเนื่องจากความเค้น นอกจาก่นี้
ฟิล์มคาร์บอนคล้ายเพชรที่ได้ยังแลดงการสะท้อนรังสีอัลตราไวโอเลตใน
ช่วงความยาวคลื่น 200-300 นาในเมตรน้อยที่สุดอีกด้วย ซึ่งผลการ
ทดลองแสดงดังรูปที่ 3

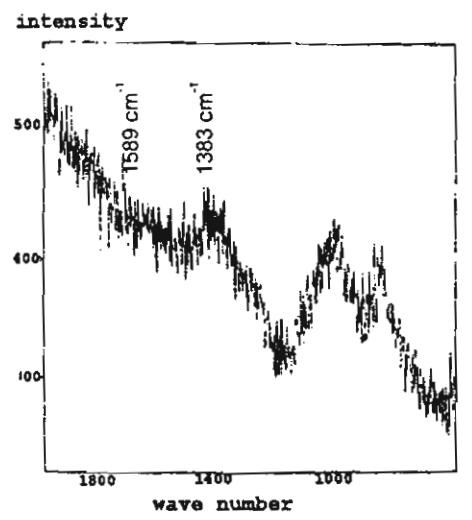
สำหรับคาร์บอนคล้ายเพชรที่ถูกเตรียมในบรรยากาศของแก็ส ไฮโดรเจนจะให้สเปกตรัมของรามานแสดงจีพีค (G-peak) ที่ 1589 เซนติเมตร ใและดีพีค (D-peak) ที่ 1383 เซนติเมตร ซึ่งแสดงถึงคุณ สมบัติที่มีความคล้ายเพชรมากกว่าคาร์บอนที่เกิดในบรรยากาคของแก็ส อาร์กอน แสดงได้ดังรูปที่ 4



รูปที่ 2 แสดงระบบสุญญากาศสำหรับวิธีสปัตเตอริงไฟฟ้ากระแลสลับ

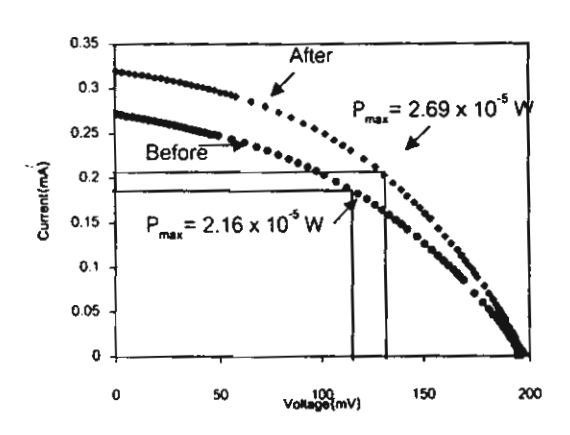


รูปที่ 3 แสดงคุณสมบัติของฟิล์มคาร์บอนคล้ายเพชรบนซิลิกอน (100)ที่เตรียมในบรรยากาศของแก๊สอาร์กอน



รูปที่ 4 แสดงสเปกตรัมของรามานของคาร์บอนคล้ายเพชรบนซิลิกอน ที่เตรียมในบรรยากาศของแก๊สไฮโดรเจน

2. คาร์บอนคล้ายเพชรบนเซลล์แลงอาทิตย์ที่มีพื้นที่ 0.98 เซนติเมตร<sup>2</sup> ถูกเตรียมที่ความคัน 60-70 มิลลิทอร์ ในบรรยากาศของ แก๊สอาร์กอนเป็นเวลา 1 ชั่วโมง ซึ่งฟิล์มคาร์บอนคล้ายเพชรที่ได้มีคุณ สมบัติในการคูดกลืนรังสีอัลตราไวโอเลตได้ดีจึงทำให้เซลล์แลงอาทิตย์มี ประสิทธิภาพเพิ่มขึ้นจาก 5.5 เป็น 7.0 (เพิ่มขึ้นร้อยละ 27.3) สุณสมบัติของกระแสไฟฟ้าและแรงคันไฟฟ้าแสดงดังรูปที่ 5



รูปที่ 5 แสดงคุณสมบัติของกระแสไฟฟ้าและแรงคันไฟฟ้า ของเซลล์แสงอาทิตย์ที่มีพื้นที่ 0.98 เซนติเมตร<sup>2</sup>

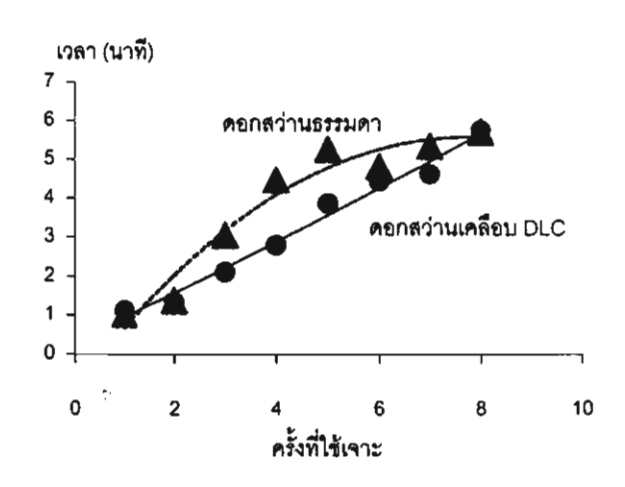
สำหรับเขลล์แสงอาทิตย์อีกขึ้นหนึ่งที่มีพื้นที่ 4.05 เซนติเมตร<sup>2</sup> ที่ทำการเคลือบคาร์บอนคล้ายเพชรมีประสิทธิภาพเพิ่มขึ้นเป็น 6.6 จาก เดิม 6.5 (เพิ่มขึ้นร้อยละ 1.5) จะเห็นว่าถึงแม้พื้นที่ในการรับแสงของตัว อย่างนี้มีมากกว่าตัวอย่างแรกแต่เนื่องจากพื้นที่ที่ทำการเคลือบด้วย

คาร์บอนคล้ายเพชรไม่สม่ำเสมอทั่วทั้งแผ่นจึงทำให้มีการเพิ่มประสิทธิ ภาพไม่มากนัก

3. คาร์บอนคล้ายเพชรถูกเตรียมบนคอกสว่านที่มีเส้นผ่าศูนย์
กลางขนาด 5 มิลลิเมตร ที่ความคัน 200 มิลลิทอร์ ในบรรยากาศของ
แก็สอาร์กอนเป็นเวลา 2 ขั่วโมง แล้วนำมาทด่สอบด้วยการเจาะแผ่น
เหล็กที่มีความหนา 5 มิลลิเมตร โดยใช้แรง 50 นิวตันและจับเวลาใน
การเจาะทะลุผ่านแผ่นเหล็กในแต่ละครั้งซึ่งได้ผลการทดลองดังตารางที่ 1
พบว่าดอกสว่านที่ผ่านการเคลือบคาร์บอนคล้ายเพชรใช้เวลาในการเจาะ
ทะลุแผ่นเหล็กในแต่ละครั้งน้อยกว่าดอกสว่านที่ไม่ได้ทำการเคลือบแสดง
ดังรูปที่ 6 ซึ่งแสดงให้เห็นถึงการประหยัดเวลาและพลังงานในการเจาะ
ของดอกสว่านที่ผ่านการเคลือบด้วยคาร์บอนคล้ายเพชรใต้เป็นอย่างดี

ตารางที่ 1 แลดงการเปรียบเทียบเวลาที่ดอกสว่านใช้ในการเจาะทะลุ แผ่นเหล็กหนา 5 มิลลิเมตร

ครั้งที่	เวลาที่ดอกสว่านใช้ในการเจาะทะลุ แผ่นเหล็กหนา 5 มิลลิเมตร (นาที)				
	คอกสว่านธรรมดา	ดอกสว่านที่เคลือบด้วย คาร์บอนคล้ายเพชร			
1	1.03	1.13			
'					
2	1.38	1.34			
3	3.06	2.12			
4	4.47	2.80			
5	5.27	3.86			
6	4.82	4.43			
7	5.35	4.62			
8	5.72	5.76			



รูปที่ 6 แสดงความลัมพันธ์ระหว่าง เวลาที่เจาะทะลุแผ่นเหล็ก กับ ครั้งที่ ใช้เจาะของดอกสว่านธรรมดาและดอกสว่านเคลือบ DLC

สรป

การเคลือบวัสคุด้วยคาร์บอนคล้ายเพราด้วยวิธีสปัตเตอริงจากไฟฟ้า
กระแสสลับร่วยเพิ่มคุณสมบัติที่คีขึ้นแก่วัสดุ ซึ่งเห็นได้จากบระสิทธิภาพ
ที่เพิ่มขึ้นของเซลล์แสงอาทิตย์ที่ทำการเคลือบด้วยคาร์บอนคล้ายเพรร
เพิ่มขึ้นถึงร้อยละ 27.3 แต่ยังพบปัญหาความไม่สม่ำเสมอของคาร์บอน
คล้ายเพราสำหรับพื้นที่บริเวณกว้าง ดอกสว่านที่ทำการเคลือบด้วย
คาร์บอนคล้ายเพราใช้เวลาในการเจาะเหล็กหนา 5 มิลลิเมตรน้อยกว่า
คอกสว่านธรรมดา เปรียบเทียบในการเจาะครั้งที่เดียวกัน ตามที่แสดงใน
รูปที่ 6 จะพบว่าการเจาะครั้งที่ 1- 2 ใช้เวลาไม่ต่างกัน ส่วนครั้งที่ 3 - 7
นั้นใช้เวลาน้อยลงอย่างเห็นได้รัด สำหรับดอกสว่านเคลือบ DLC จน
กระทั่งการเจาะครั้งที่ 8เป็นต้นไปใช้เวลาไม่ต่างกัน แสดงว่า DLC ที่
เคลือบคงหลุดออกเป็นส่วนมากแล้ว ซึ่งเป็นปัญหาที่ต้องปรับปรุงต่อไป
ในคุณสมบัติการยึดแน่นของ DLC บนดอกสว่าน ผลการทดลองทั้งสอง
แสดงให้เห็นว่าสามารถนำคาร์บอนคล้ายเพราไปประยุกต์ใช้ในชีวิต
ประจำวันได้

เอกสารอ้างอิง

- Windischmann H, Gray KJ. Stress measurement of CVD diamond films. Diamond and Related Materials 1995; 4: 131-141.
- Knight Diane S, White William B. Charecterization of diamond films by Raman spectroscopy. Journal of Materials Research 1989; 4(2): 385-393.
- 3. สมศักดิ์ ปัญญาแก้ว. เทคโนโลยีเซลล์แลงอาทิตย์. สำนัก พิมพ์แห่งจุฬาลงกรณ์มหาวิทยาลัย กรุงเทพมหานคร 1983.



# บทคัดย่อ EXTENDED ABSTRACTS

การประชุมวิชาการ

วิทยาศาสตร์และเทคโนโลยีแห่งประเทศไทย ครั้งที่ 28

24-26 ตุลาคม 2545 ณ ศูนย์การประชุมแห่งชาติสิริกิติ์ กรุงเทพฯ

28th Congress on Science and Technology of Thailand

24-26 October 2002

Queen Sirikit National Convention Center, Bangkok



สมาคมวิทยาศาสคร์แห่งประเทศไทยในพระบรมรารูปถัมภ์, THE SCIENCE SOCIETY OF THAILAND UNDER THE PATRONAGE OF HIS MAJESTY THE KING



คณะวิทยาศาสตร์ประยุกด์ สถาบันเทคในใสยีพระจอมเกล้าพระนครเหนือ FACULY OF APPLED SCIENCE,

KING MONGKUTS INSTITUTE OF TECHNOLOGY NORTH BANGKON

วิทยา อมรกิจบ้ารุง และ องค์อร ตอพล

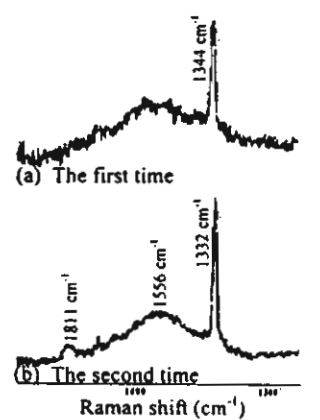
Vittaya Amonkitbumrung and Ong-on Topon

Department of Physics, Faculty of Science, Khon Kean University; ong-on@hotmail.com

บทลัดย่อ. การปลูกผลึกเพชรโดยอาศัยการขัดวัสดุฐานรองชิลิกอนด้วยผงเพชร แล้วนำไปปลูกผลึกด้วยกระบวนการ HFCVD (hot filament chemical vapor deposition) ที่ใช้แก๊สไฮโดรเจนและแก๊สมีเทนเป็นแหล่งกำเนิดคาร์บอนเริ่มต้น เงื่อนไซที่ใช้ในการปลูกผลึกคือ อุณหภูมิของเล้น ควดกำเนิดความร้อน 1900 – 2000 °C, อุณหภูมิที่ผิวของวัสดุฐานรอง 500 °C ปลูกผลึกเป็นเวลา 5 ชั่วโมงที่ความดัน 31 มิลลิบาร์ การวิเคราะห์ใช้ .พูคนิคการวิเคราะห์ด้วยสเปกตรัมของรามานและกล้องจุลทรรศน์แบบสองกราด ฟิล์มเพชรที่เกิดขึ้นแสดงรามานสเปกตรัมของเพชรที่ 1344 cm<sup>-t</sup> \_ละเลื่อนกลับมาที่ 1332 cm ใหลังจากเวลาผ่านไป 51 วัน และฟิล์มเพชรเกิดรอยแตก จากผลการทดลองนี้แลดงให้เห็นความเค้นที่เกิดขึ้นในฟิล์ม พระ นอกจากนี้เรายังพบความเค้นระหว่างฟิล์มกับวัสดุฐานรองเป็น 3392 GPa และ 3532 GPa ในทิศทางที่ตั้งจากกัน

Abstract: The diamond powder was used to scratch surface of silicon (100) substrate for diamond crystal growth by HFCVD (hot filament chemical vapor deposition) with H2 and CH4 gas sources. The deposition conditions were 1900 - 2000 °C of filament temperature 500 °C of substrate surface temperature, 31 mbar in pressure and 5 hour in deposition time. The Raman spectroscopy and SEM techniques were used to analyze the film. The diamond Raman spectrum was shift to 1348 cm<sup>-1</sup> and relaxed to 1334 cm<sup>-1</sup> after 51 days. The film was cracked when diamond film stress was relaxed. These results show that the diamond film has stress in the film. The stress between film and substrate was observed by XRD. The stresses are 3392 GPa and 3532 GPa in normal and parallel orientation, respectively.

Methodology: The vacuum system in pressure 10<sup>-8</sup> mbar was pumped by titanium sublimation pump and turbomolecular pump. A Si(100) wafer, p-type, specimen 10 mm x 10 mm was scratched by diamond powder, cleaned by acetone and methanol in ultrasonic for 1 hour in ultrasonic cleaner in each solvent, etched by lactic acid: HNO3: HF = 25: 4: 1 for 10 minutes and dried by dry nitrogen for a few minutes. The silicon substrate was 1-2 mm from a tungsten filament, 1900-2000 °C in temperature and was thermally cleaned with filament for 1 hour. The substrate surface temperature about 500 °C. The deposition conditions were 5 hour and 31 mbar. H<sub>2</sub> flow rate is 176 sccm and CH<sub>4</sub> flow rate is 0.44 sccm.



Result, Discussion and Conclusion: The diamond film was analyzed by Raman spectroscopy, SEM and XRD. The first order peak of standard diamond Raman spectrum was 1332 cm<sup>-1</sup> standard peak. The film showed 1344 cm<sup>-1</sup> sharp peak, crystalline diamond, and 1550 cm<sup>-1</sup> broad peak, crystalline graphite (Fig. 1a) [1]. The diamond peak was shifted 16 cm<sup>-1</sup> from standard because of stress between diamond film and silicon substrate. The film has grain size 0.3 µm and has space between grains that cause of stress [2]. After 51 days, the diamond peak was shifted to 1332 cm<sup>-1</sup> (Fig. 1b) because stress was relaxed and caused the film cracked [3]. These results showed that diamond powder scratched technique caused stress in the film. The XRD technique was used to observe stress between the film and the substrate. The substrate was orientated in normal and parallel to the X-ray that found stress 3392 GPa in normal and 3532 GPa in parallel.

Fig. 1 The Raman spectrums of diamond film.

References: (1) Tydall, George W. Hacker, Nigel P. (1989) Mat. Res. Soc. Sym. Pro. 162, 173-178.

- (2) Dowling, D. P. Ahern, M. J. Kelly, T. C. Meenan, B.J. Brown, N. M. D. O'Connor, G. M. Glyn,n T. J. (1992) Sur. Coa. Tech. 53, 177-183.
- (3) Boteler, J. M. Gfupta, Y. M. (1993) Phy. Rev. Lat. 71(21), 3497-3500.

Keywords: diamond film, silicon substrate, stress Raman spectroscopy, SEM

## Surface and quality modification of diamond-like carbon films by ${\rm CO_2}$ laser heating assisted hot filament chemical vapor deposition

### V.Amornkitbamrung and Ong-On Topon

Department of Physics, Faculty of Science, Khon Kaen University, Khon Kaen 40002, Thailand

### Abstract

An infrared CO<sub>2</sub> laser was used for regional heating to study the heating effect on HF-CVD of DLC formation on Si(100) face substrates. The micro-Raman spectrometer and scanning electron microscope were used for characterization of the chemical bonding types and surface morphology. The tungsten filament temperature was about 1850-1950 ° C. The substrate surface temperature was about 450-500 ° C. The power of the laser was varied by biasing the CO<sub>2</sub> laser tube, 30 cm long at three different input currents, 6, 7, and 8 mA which raised the temperature on the substrate locally 25, 45 and 55 °C respectively. At the medium laser power, at the central laser beam region a narrow Raman peak centered at 1438 cm<sup>-1</sup> was detected. It can be concluded that this region has good quality DLC. This moderate high frequency peak corresponds to the four-fold rotation symmetry atom in amorphous carbon network from the tight-binding molecular dynamic simulation of C.Z. Wang and K.M. Ho. The SiC Raman sharp peak at 765 cm<sup>-1</sup> was observed which should be a phase at the interface between DLC film and Si substrate. We observed this interface region in the cross-sectional SEM image. In the Raman spectrograph a small peak at about 1080-1090 cm<sup>-1</sup> was observed, which may be nanocrystalline diamond phase corresponding to some nano-DLC particles observed by SEM.

Keywords: DLC; Laser heating; Raman spectroscopy; SEM; UV-VIS

### 1. Introduction

Diamond is a material which has unique properties better than other materials in many ways such as optical transparency from X-rays to infrared radiation, high thermal conductivity five times that of copper, inert to chemical agents, extreme hardness and can withstand radioactivity. It is a good insulator, but it can be doped to become a semiconductor for device applications in an aggressive corrosion, high temperature and high radiation environment.

Diamond-like carbon(DLC) is an amorphous form of carbon which has hydrogen in a carbon tetrahedral matrix. The DLC is very interesting because it has comparable properties with diamond. The DLC thin film preparation has been successful since high vacuum technology was developed for thin film deposition. DLC thin films are normally composed of sp<sup>2</sup> (graphite phase) and sp<sup>3</sup> (diamond phase) mixed bonding due to the hydrogen content in the thin film.

There have been attempts in using lasers to assist chemical and physical vapor deposition processes for improvement of homogeneity, adhesion to substrate, surface smoothness, structure, deposition rate, electrical and optical properties of diamond and DLC production [1-9]. There have been some attempts in using pulsed-laser ablation of graphite for induced transformation of graphite to diamond via an intermediate rhombohedral graphite [10] and for homoepitaxial growth of diamond in oxygen atmosphere[11].

In this research we used an infrared CO<sub>2</sub> laser for regional heating to study the heating effect on HF-CVD of DLC and diamond formation on Si(100) face substrates. The micro-Raman spectrometer, scanning electron microscope and UV-visible spectrophotometer were used for characterization of the chemical bonding types, surface morphology and optical transparency.

### 2. Experimental

A Si(100) wafer, p-type, 1 inch in diameter and 0.30 mm in thickness, was sectioned into specimens 10 mm x 10 mm and cleaned with acetone and methanol in an ultrasonic cleaner for 1 hour in each solvent, rinsed with deionized water and dried with dry nitrogen for a few minutes. The silicon substrate was loaded into the load-lock system and manually transferred into the ultra high vacuum chamber at a pressure of 10<sup>-8</sup> mbar,

evacuated by means of combined titanium sublimation and turbomolecular pump as shown in the diagram of the system in Fig.1. The silicon substrate was about 1-2 mm from a tungsten filament circular coil and the substrate was "in situ" thermally cleaned with the hot filament for 1 hour. The filament temperature was about 1850-1950 °C, detected by optical pyrometer. The substrate surface temperature was about 450-500 °C, detected by the chromel-alumel thermocouple. A CO<sub>2</sub> laser beam, 2 mm in diameter, continuous wave, was used to heat the substrate for a further 20 minutes. Ultra pure H<sub>2</sub> was flowed into the chamber with a flow rate of about 200-215 sccm, followed by flowing CH<sub>4</sub> gas with a flow rate of about 0.40-0.50 sccm. The power of the laser was varied by biasing the CO<sub>2</sub> laser tube 30 cm long at three different input currents, 6, 7 and 8 mA which raised the temperature of the substrate locally 25, 45 and 55 °C respectively. These raising temperatures were calculated by the heat conduction equation [12]. The three different laser powers were called low, medium and high power heating conditions for the three different input currents, 6, 7 and 8 mA respectively. The deposition conditions were 5 hours and 21-25 mbar in pressure. These samples were characterized by micro-Raman spectrometer, scanning electron microscope and UV-visible spectrophotometer.

### 3. Results and discussion

In the low power laser heating condition, there are DLC, mainly graphite-like carbon and  $\beta$ -SiC phases as observed on Raman spectrograph as shown in Fig.2a. The  $\beta$ -SiC peaks are at 781, 959 cm<sup>-1</sup> compared with the  $\beta$ -SiC standard peaks of 796, 973 cm<sup>-1</sup> ( $\Delta \nu$ =-14,-15 cm<sup>-1</sup>;  $\Delta \nu$ = $\nu_o$ - $\nu$ ;  $\nu_o$  is the standard wave number,  $\nu$  is the observed wave number) which may come from tensile stress of  $\beta$ -SiC heteroepitaxial thin film on Si substrate. The D-peak (1362 cm<sup>-1</sup>) and G-peak (1579 cm<sup>-1</sup>) are the same as the G and D standard peaks (1360 and 1580 cm<sup>-1</sup>) and these phases are independent of the substrate structure.

In the medium power laser heating condition, the single narrow Raman peak of FWHM about 300 cm<sup>-1</sup> centered at 1438 cm<sup>-1</sup> was observed as shown in Fig.2b. This peak has more intensity than the D-peak (1362 cm<sup>-1</sup>) and G-peak (1579 cm<sup>-1</sup>) which were observed in the low power laser heating condition. This is the first time in observing a quite sharp peak of 1438 cm<sup>-1</sup> from the moderate laser power heating on the substrate surface during HFCVD of DLC on Si. This peak was predicted by using tight-binding molecular-dynamic (TBMD) simulation[13]. The TBMD scheme was used to generate diamond-like amorphous carbon structure by quenching high-density carbon liquid from high temperatures. The simulation parameters such as carbon density, temperature, cooling rate, annealing process are comparable with the experimental condition. The simulation concluded that these high frequency modes (between 1300-1500 cm<sup>-1</sup>) came from the stretching vibrations between the fourfold and threefold atoms, and between fourfold sites when bond angles are severely distorted. It was found that this mode was relatively localized with 20-30% of the vibrational amplitudes on a pair of atoms. It correspond to our experiment results of this peak which was observed only from the exact center of the laser beam region.

In the high power laser heating condition, there are two broad bands of Raman spectrograph centered at 1378 cm $^{-1}$  and 1752 cm $^{-1}$  as shown in Fig.2c. These peaks should come from the distortion of D and G peaks due to high temperature. It is confirmed by observing the two  $\beta$ -SiC peaks were broadened and overlapped, becoming a broad peak centered at 815 cm $^{-1}$ .

The SEM from top view and cross section of three different laser powers are shown in Fig. 3a-c and Fig.4a-c respectively. In the low power laser heating condition, the particles of DLC, graphite-like carbon and  $\beta\text{-SiC}$  are quite nearly the same size of about 120 nm. These particles are distributed homogeneously in the central laser beam region. In the medium power laser heating condition, there are DLC and  $\beta\text{-SiC}$  particles at nearly the same size of about 200 nm. These particles agglomerated in each group but are clearly separated in each particle in the central beam region. In the high power laser heating condition, there are DLC and  $\beta\text{-SiC}$  particles of nearly the same size of about 250 nm.

The deposition rates and grain sizes of thin films in three different laser powers are shown in Fig.5 (the left axis is the deposition rate, the right axis is the grain size). The deposition rate decreased when the laser power increased. This result contradicts with the former results of other researches when the substrates were heated from the back side by a resistive heater. In this experiment, the thermal energy on the substrate surface from the

laser had the effect of fusing small grain size particles in forming the big grain size particles, and therefore the deposition rate decreased.

The UV-visible transmission of three different laser powers DLC thin films in wavelength range 200-1100 nm are shown in Fig.6. The transmission of DLC under medium power laser heating condition are better than under high power laser heating condition. This is because the medium power laser heating condition gave the best quality DLC.

### 4. Conclusions

At the central laser beam region, the single narrow Raman peak of FWHM about 300 cm<sup>-1</sup> centered at 1438 cm<sup>-1</sup> (Fig.2b) of the medium laser power condition has more intensity than the D-peak(1362cm<sup>-1</sup>) and G-peak(1579cm<sup>-1</sup>) which were observed at the central laser beam region of the low laser power condition (Fig.2a). It can be concluded that this region of the medium laser power condition gives good quality DLC. This high frequency narrow peak at 1438 cm<sup>-1</sup> corresponds to the four-fold rotating symmetry atom in amorphous carbon network from the tight-binding molecular dynamic simulation of [13]. This narrow peak at 1438 cm<sup>-1</sup> may compare with the broad peak at 1465 cm<sup>-1</sup> from fullerences in carbon foam[14] and may compare with sharp peaks at 1422, 1447,1467 cm<sup>-1</sup> from defect structure in diamond implanted with MeV He ions, [15]. In the Fig. 2b and 2c of Raman spectrograph there is a peak at about 1080 and 1090 cm<sup>-1</sup> which may be the nanocrystalline diamond phase which corresponds to the nano-DLC particles observed by SEM. The SiC Raman sharp peak at 765 cm<sup>-1</sup> (Fig.2b) should be the interface phase between DLC film and Si substrate. We observed this interface region in the cross-section SEM image in Fig. 4b. Another SiC peak at 909 cm<sup>-1</sup> (Fig.2b) interfered with the second order Si square topped peak which usually is at about 950 cm<sup>-1</sup>. These peaks shifted from the standard β-SiC Raman peaks at 796 and 973 cm<sup>-1</sup> [16], which should come from the stress formation between Si substrate and DLC thin film or these peaks may be the \alpha-SiC Raman peaks.

The central laser beam regions at the three laser power conditions can be compared from Raman spectrographs among Fig.2a, 2b and 2c. It can be concluded that the low laser power condition is the initial state of DLC formation. In the initial state of DLC formation; G-, D- and  $\beta$ -SiC peaks appeared at the same time which implied graphite-like, disordered carbon and  $\beta$ -SiC assisted DLC formation on Si. In the medium laser power condition in which the substrate temperature is higher than the low laser power condition by about 20  $^{\circ}$ C, the broad Raman peak at about 1480 cm $^{-1}$  was observed. There is a very narrow temperature range[17], 490-495  $^{\circ}$ C, for high ordering of carbon formation similar to defect structures in diamond. It may be called amorphous diamond in our work.

In DLC deposition by laser assisted HFCVD, the temperature affected the purity of the DLC phase and made the surface more homogenous. The homogenous DLC deposition condition for coating on Si substrate may be applied for increasing solar cell efficiency[18]. There are two reasons for this effect i.e. DLC absorbed UV spectrum and emission of visible light to enhance the silicon solar cell efficiency. Another reason should be the DLC particle size which corresponds to UV wavelength of about 200 nm. It can absorb UV more than other sizes. This application should be used in the near future.

### Acknowledgement

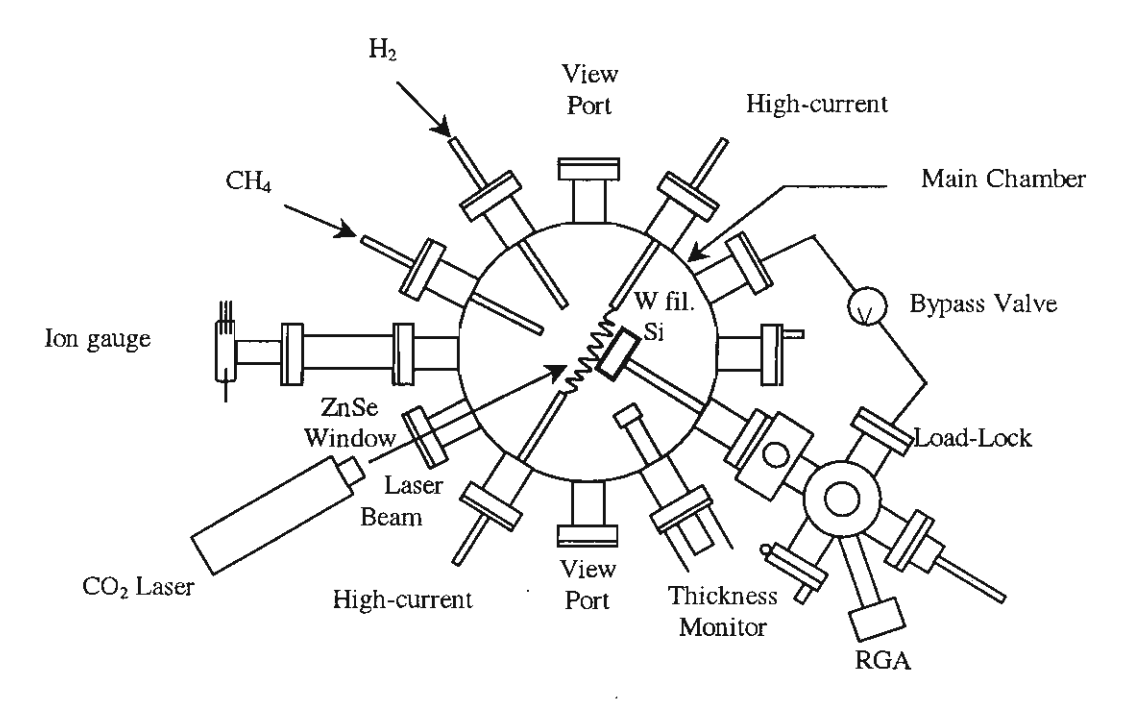
This work was supported by the Thailand Research Fund (TRF) under contract no. RSA/19/2543.

### References.

- [1] S. Fujimori, T. Kasai and T. Inamura, Thin Solid Films, 92(1982) 71.
- [2] G. W. Tyndall and N. P. Hacker, Symp. on Diamond, Silicon Carbide and Related Wide Bandgap Semiconductors, November 27-December 1, 1989, Boston, Massachusetts, U.S.A., Materials Research Society Symposium Proceeding, 162(1989) 173
- [3] P. E. Pehrsson, H. H. Nelson and F. G. Celii, Symp. on Diamond, Silicon Carbide and Related Wide Bandgap Semiconductors, November 27-December 1, 1989, Boston, Massachusetts, U.S.A., Materials Research Society Symposium Proceeding, 162(1989) 179.

- [4] A. Rengan, N. Biunno and J. Narayan, Symp. on Diamond, Silicon Carbide and Related Wide Bandgap Semiconductors, November 27-December 1, 1989, Boston, Massachusetts, U.S.A., Materials Research Society Symposium Proceeding, 162(1989) 185.
- [5] S. M. Metev, M. Ozegowski, K. Meteva, G. Sepold, T. V. Kononenko, V. I. Konov, E. D. Obraztsova, S. M. Pimenov, V. G. Ralchenko and A. A. Smolin, Diamond Relat. Mater., 2(1996) 420.
- [6] S. E. Johnson, M. N. R. Ashford, M. P. Knapper, R. J. Lade, K. N. Rosser, N. A. Fox, Diamond Relat. Mater., 6(1997) 569.
- [7] M. Lindstam, M. Boman and J. O. Carlsson, Appl. Surf. Sci., 109/110(1997) 462.
- [8] A. Badzian, B. L. Weiss, R. Roy, T. Badzian, W. Drawl, P. Mistry and M. C. Turchan, Diamond Relat. Mater., 7(1998) 64.
- [9] V. I. Konov, A. M. Prokhorov, S. A. Uglov, A. P. Bolshakov, L. A. Leontiev, F. Dausinger, H. Hugel, B. Angstenberger, G. Sepold and S. Metev, Appl. Phys. A, 66 (1998) 575.
- [10] G. W. Yang and J. B. Wang, Appl. Phys. A, 72(2001) 475.
- [11] T. Yoshitake, T. Nishiyama and K. Nagayama, Jpn. J. Appl. Phys. 40(2001) L573.
- [12] Q. Wang, R.Schliesing, H. Zacharias and V. Buck, Appl. Surf. Sc.138-139(1999) 429.
- [13] C.Z. Wang and K.M. Ho, Phys. Rev. Lett.,71(1993)1184.
- [14] A. V. Rode, E. G. Gamaly and B. Luther-Davies, Appl. Phys. A, 70(2000) 135.
- [15] S. Prawer, K. W. Nugent and D. N. Jamieson, Diamond Relat. Mater., 7(1998) 106.
- [16] B. R. Stoner and J. T. Glass, Appli. Phys. Lett., 60(1992)698.
- [17] S. Rey, F. Antoni, B. Prevot, E. Fogarassy, J. C. Arnault, J. Hommet, F. Le Normand and P. Boher, Appl. Phys. A, 71(2000) 433.
- [18] V.G. Litovechenko and N.I. Klyui, Solar Energy Mater. 68(2001) 55.

### Plan view



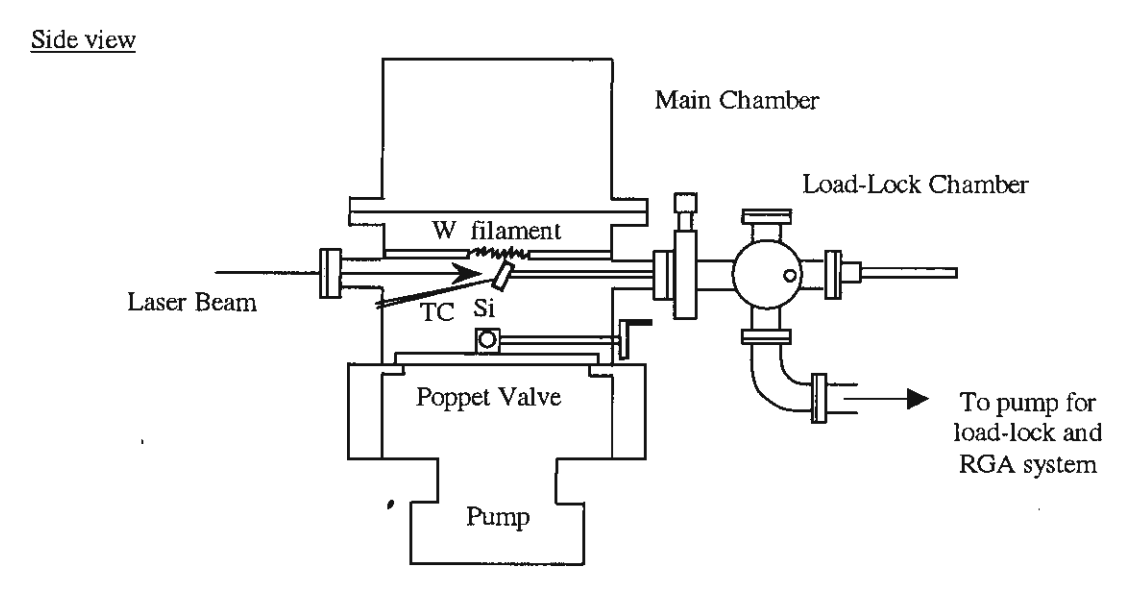


Fig. 1. Plan and side views of CO<sub>2</sub> laser heating assisted HF-CVD system

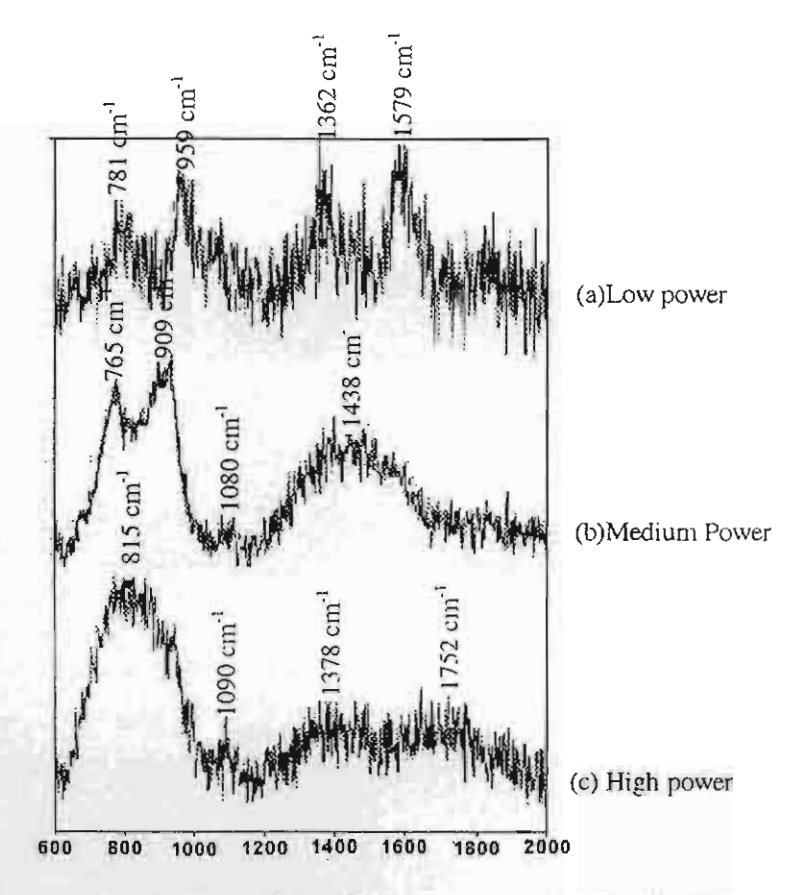


Fig. 2 Raman spectra for three different laser power densities at the center.

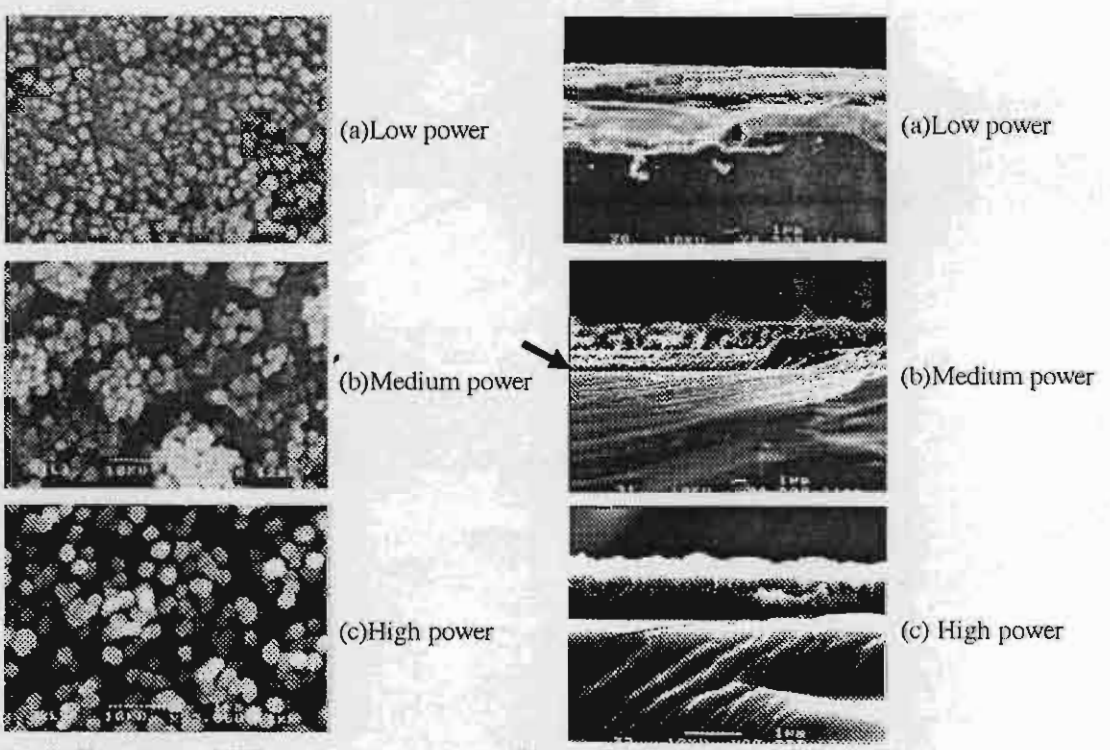


Fig. 3 Top view of different laser power densities at the center by SEM.

Fig. 4 Cross-section of different laser power densities at the center by SEM. Arrow in (b) indicates the interface.

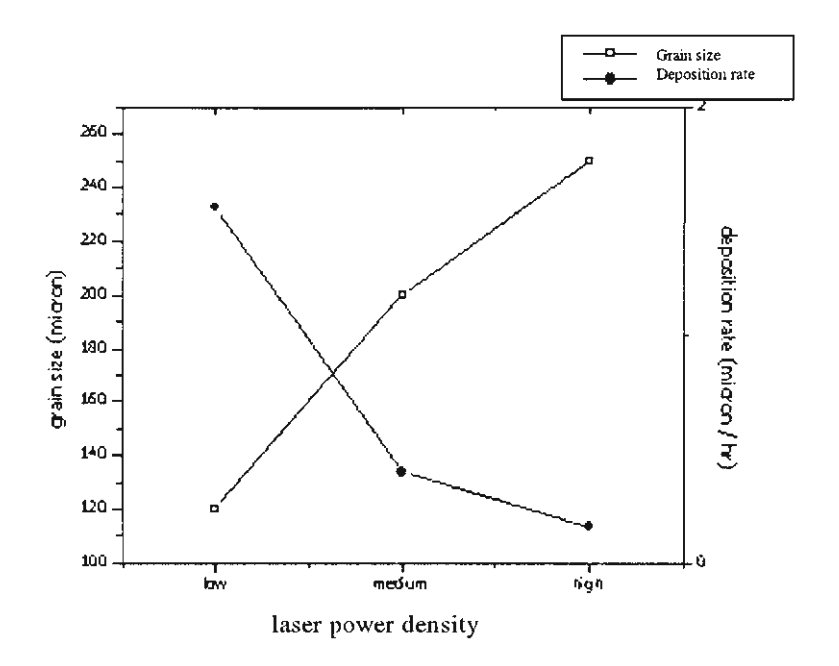


Fig. 5 Deposition rates and grain sizes for different laser power densities at center

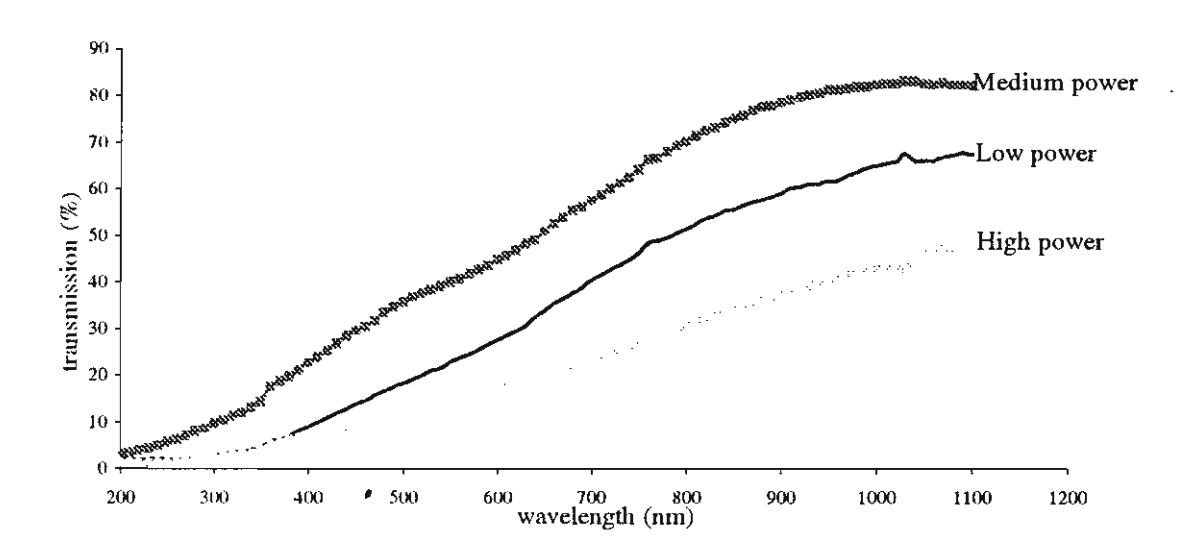


Fig. 6 UV visible transmission for different laser power densities at center.